WORKING PAPER · OCTOBER 2026 · REVISION 10.2 · PARTS I AND II

Geometry of a Three-Orb Metastructure

A kinematic reconstruction of circulating luminous objects in publicly circulated aircraft footage, with the dynamics it implies

Bryan M. Ingram
Advanced Energy & Frontier Technology
www.bryaningram.com

Part I: Geometry, dynamics and tests · Part II: Candidates, mechanisms and open questions

This paper reconstructs the geometry implied by circulating-orb sequences associated with the MH370 video corpus, and works out the forces that geometry would require. It is a model of path and formation, not an authentication of the footage and not a claim that a wormhole was observed.

Abstract

Publicly circulated electro-optical and thermal sequences associated with the so-called MH370 orb corpus show three compact luminous objects moving in coordinated fashion about a wide-body airframe. Treating those objects as real point masses for the purpose of reconstruction — and stating the published counter-evidence on provenance rather than remaining silent on it — this paper writes down the simplest geometry that fits the reported kinematics: a rigid equilateral triad locked at 120° and rotated about the fuselage axis, optionally riding a thin toroidal envelope. With an orbital radius scaled to a 777-class airframe at r = 42 m, the triad has side length $s = r\sqrt{3} \approx 72.7$ m. Circumferential speed is $r\omega$. A weak axial oscillation turns each circular orbit into a flattened helix on the torus, which is the geometric content of the “donut / standing-wave” language used in commentary on the clips. Part I adds the dynamics the kinematics imply: the centripetal requirement and the sign of the coupling it demands, the instability of a passively bound equilateral triad, the spin-up that angular-momentum conservation forces on any collapse, an order-of-magnitude bound on a magnetic binding, the aerodynamic and radiometric budgets, and the energy scale of the “portal” reading. In Part II three candidates are costed against those requirements, a spherical inertial-electrostatic device, a pulsed Z-pinch and a buoyant microwave-sustained plasmoid, the means by which such objects could be steered are examined, the relativity of separated wormhole mouths is reviewed, and a programme of experiments is set out. The model is offered as a measurement frame, not as proof of exotic propulsion.

How the paper is organised. Part I (§§1–8) is the core: what the footage is and is not, the geometry, the dynamics that geometry implies, and the measurements that would confirm or break it. It can be read alone and asks the reader to accept nothing beyond mechanics. Part II (§§9–17) is a companion. It takes the mechanisms that have been proposed for the objects — plasmoids, the Navy filings, three candidate cores, steering by fields, software and intention, and the relativity of separated wormhole mouths — and costs each against the requirements of Part I, keeping what survives. It ends with a programme of work and a closing. Section, equation, figure and reference numbers run continuously through both parts.

Note on this release (Revision 10.2). Revision 10.2 incorporates a formal mathematical review and rebuild of this paper by Nathanael J. Bocker [40], carried out under his MAPEOGEOv2 certification and PSMSL observability framework. His audit passed the kinematic core and reproduced the numerical estimates, and found four places where a correct equation had been asked to carry a stronger conclusion than it licenses: the toroidal perturbation of Equation 5 (now split into two branches, Equation 5b); the stability claim of §7.2 (now stated as mechanism-dependent, Equation 7b); the collapse kinematics of Equation 9 (now completed with the radial terms and the tilted invariant, Equation 9b); and a factor-of-two convention in the throat benchmark of §11.4. Each is corrected in place and marked. His observability hierarchy is adopted in §8. None of it changes the paper’s conclusions; it narrows the central claim to what the mathematics supports. This paper is the test case of the first in a series of open analyses of theories of everything. The frustration behind the series is that such theories usually stop at the equations: there is rarely a worked example, a current technology the theory speaks to, a derivation a peer can check line by line, or an exercise a student can change a number in and watch. This release therefore pairs the paper with a technical supplement, *The Scaled-Metric Reading*, which adopts five postulates distilled from Dr. Norbert Schwarzer’s scaled-metric framework (*Fluid Universe: The Way of Structured Water and its Mathematical Foundations*, Jenny Stanford Publishing, 2026) and re-derives this paper under them; a plain-language guide, *The Seam*; an interactive console in which the formulas can be turned by hand; and a hardware design study published for critique. Dr. Schwarzer reviewed an earlier revision of this paper, and his comments on dimensionality and scale prompted §7.7 and the exercise; he has not reviewed the supplement, the guide or the console, and any error in reducing his framework is the author’s. None of it is a claim that the framework is right or that the footage is real. It

is an invitation to check the mathematics and to say where it breaks.

PART I

Geometry, dynamics and tests

What the sequences show, the path and formation they imply, the forces that path would require, and the measurements that decide it.

1. Purpose and limits
2. What the sequences appear to show
3. Coordinate frame
4. The path
5. The triangle
6. The torus — the donut envelope
7. Dynamics implied by the kinematics (with 7.7, dimensionality and scale)
8. What would confirm or break the model

1. Purpose and limits

Geometry is prior to interpretation. Before one argues fusion confinement, magnetic reconnection, or topology change, one should be able to say where the objects are, how they move relative to the airframe, and what invariants the formation keeps. The first half of this paper attempts that. The second half asks the next question a physicist would ask: what forces would hold such a path, and what do those forces predict that a drawing does not.

Two limits are binding. First, the clips in circulation have not been authenticated as original sensor records; stereo disparity, platform motion, and compression artifacts remain open, and specific counter-evidence is on the record (§1.1). Second, nothing in a path equation establishes a power source. Field-reversed configuration (FRC) plasmoids and polyhedral cusp confinement are discussed only as the nearest published laboratory geometries that produce self-organized luminous spheres and triangular force-free arrangements — an analogy, not an identification.

The reconstruction is therefore conditional: *if* three compact objects circle a wide-body jet as the sequences depict, *then* the path and the metastructure have the form written below. Falsification is welcome and specified in §8.

1.1 Published counter-evidence

A paper that invites falsification should state what has already been offered. Three items are on the record. First, in August 2023 online analysts matched the terminal flash to a commercial visual-effects element: a shockwave from the Pyromania stock library, first sold on CD-ROM in the 1990s. The initial match covered a single frame and needed distortion to align; proponents call it incomplete, critics call it decisive. Second, in December 2023 the cloud field in the satellite-view clip was matched to stock photographs on textures.com, taken from an airliner near Mt Fuji in 2012 by the artist Jonas De Ro, who has said the images are his. Ashton Forbes disputes the direction of that inference and notes that it does not address the thermal clip. Third, the conventional record is not empty: the Inmarsat handshake sequence defines a final arc in the southern Indian Ocean, and a flaperon recovered on Réunion on 29 July 2015 was identified by French investigators as belonging to 9M-MRO, with further debris recovered on western Indian Ocean shores since [18, 19].

This paper’s position follows from its conditional. If the cloud match stands, the satellite-view clip is a composite and the geometry below describes an animation. In that case the dynamics of §7 are the quickest way to show it, because an animator keys positions, not forces, and a keyed path has no reason to conserve angular momentum. If the match fails, the same tests apply to a real volume. Either way the counter-evidence belongs in the first section and not in a footnote.

2. What the sequences appear to show

Across the optical and thermal cuts most often cited in this corpus, three features recur:

- Three compact sources, not one, with apparent angular size well below the airframe.
- Coordinated motion rather than independent drift — the objects keep a mutual spacing while the jet translates.
- A change of mode: an approach or intercept, a circumferential “tune” of order one full rotation, then a tightening or vertical lock immediately before the terminal flash.

Commentary around the clips — notably the analyses gathered by Ashton Forbes and the 4ORBS archive — describes the circumferential phase as a donut or standing-wave wrap about the fuselage, and the locked phase as a triangle whose magnetic pressure then fails inward. Those words already imply a specific manifold. The next

sections write it.

Plates I and II are stills pulled from sequences circulating on X in 2026, including the thermal cut in which three compact sources hold station about a wide-body jet (@AshtonForbes, 18 September 2026) and the overhead optical family that shows an airframe, a contrail, and three point sources at once. They are reproduced here as geometric reference, not as authenticated sensor records. HUD-style brackets and corner timestamps visible in several frames are part of the circulating files.

Plate I. Thermal / FLIR stills from the circulating corpus

Public sequences as posted to X, 2026. Used here as geometric reference only.

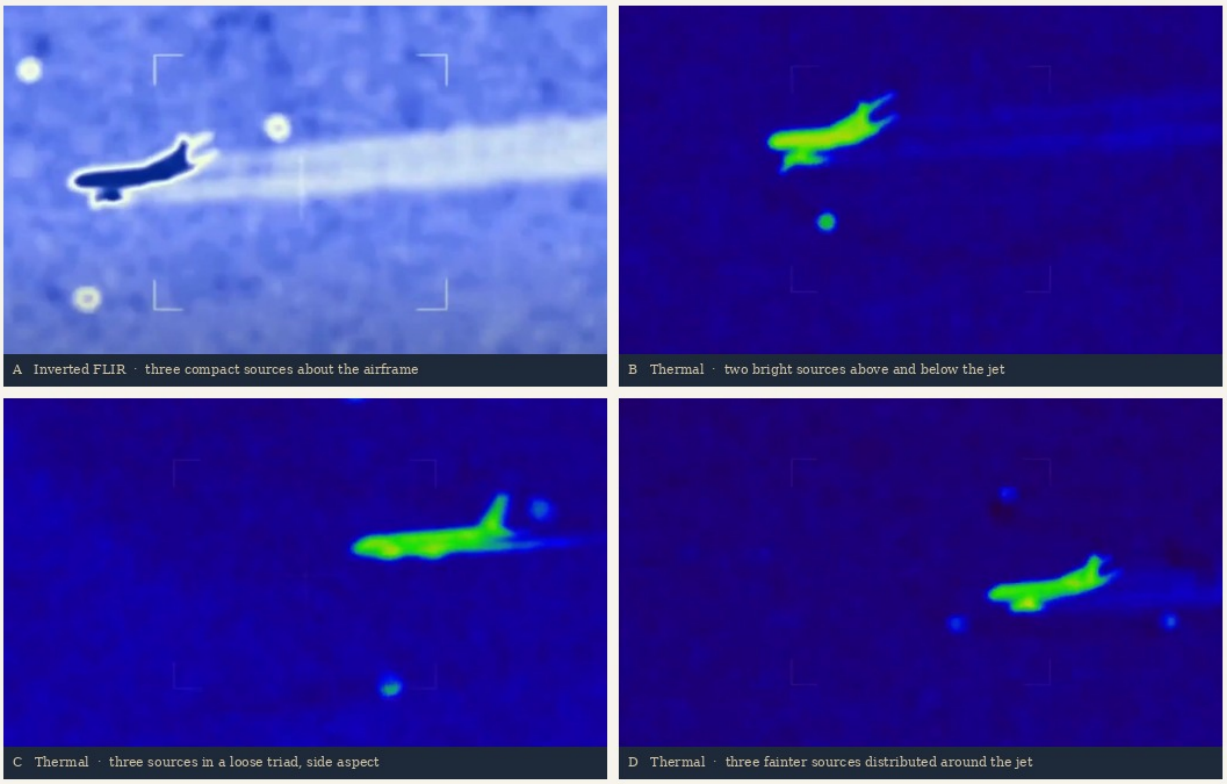


Plate I. Thermal and inverted-FLIR stills. Panel A is the clearest three-source lock in the circulating set. Panels B–D show the same class of compact sources changing station about the airframe — the motion the triad model is written to fit.

Plate II. Overhead optical stills from the circulating corpus

HUD timestamp visible at lower left in several frames of this family.



Plate II. Overhead optical stills from the same corpus family. Panel E is the frame in which an airframe, a contrail, and three compact sources are simultaneously visible. Panel F is the cloud-deck context shot used throughout the optical cuts.

A second circulating military-night-vision file is included because it is the clip most often paired with the MH370 triad in 2025–2026 commentary, and because a senior Ukrainian defence advisor publicly attached the same six-fold morphology to Armed Forces drone collection. On 11 May 2026 the account @airsuperiorx posted an 87-second monochrome sequence labelled “UAP over Ukraine in May of 2025.” The HUD in the file reads AIR / TYPHOON. A compact source is tracked against cloud, then resolves on a close pass into a bright core with six radial lobes and a warm axial plume; a conventional airframe and a second compact body appear in other frames (Plate III A–C).

Separately, and on the record, Serhiy “Flash” Beskrestnov — advisor to Ukraine’s Ministry of Defence on unmanned systems — published drone video in May 2026 of a rounded object with six pointed cones and a heat plume, recorded by an Unmanned Systems Forces pilot at about 800 m during combat operations. That is the official Ukrainian attachment of this shape to AFU collection. It is not a chain of custody for the TYPHOON-HUD file. A different, earlier AFU corpus is already in the open literature: Mavic 3T thermal records from 2023–2024 of four- and five-sphere formations that are bright in 8–14 µm and dark in the co-bore optical camera. Those spheres travel in a line or a wedge. They do not lock at 120° about an airliner, and they do not show six radial lobes. They belong in the same footnote as the May 2025 star: compact luminous sources under military sensors, different symmetry.



Plate III. Circulating May 2025 night-vision sequence. Stills from the 87-second source file posted by @airsuperiorx.

2.1 The 2026 official releases

Since 8 May 2026 the Department of War has published declassified files on unidentified anomalous phenomena at war.gov/UFO, under the Presidential Unsealing and Reporting System for UAP Encounters (PURSUE). The sixth release, on 18 September 2026, brought the series to several hundred documents, videos and recordings from the Department, AARO, the FBI, the CIA and others. The Department describes the cases as unresolved, meaning that no definitive determination could be made. That is a statement about data, not about origin, and the distinction is old: in a March 1952 talk included in the sixth release, Captain Edward Ruppelt put the residue of good reports from which no conclusion could be drawn at about one in five [29].

Three things in the releases bear on this paper, and one absence. The absence first. The coverage of the six releases consulted for this paper mentions no file that addresses MH370, and none that shows compact sources locked about an airliner; a search of the primary files should confirm that before it is relied on. The releases neither authenticate the clips of Plates I–II nor speak against them; §1.1 stands as written.

What they do supply is official sensor record of the *class*. A 2021 intelligence report on an AC-130J sortie over the Gulf of Oman logs some 25 instances of small dark orbs about 1.2 m across, moving at 250 to 1300 mph in changing formations, and notes that they were cold in the infrared. A 2025 infrared video shows six small spheres over a U.S. military platform at roughly 480 mph, changing direction frequently. Other files show four objects in formation near Iran in 2022 and a larger orb releasing smaller ones. Independent analysts have read several of these videos as small distant infrared features seen with heavy parallax from a moving platform, and that reading has to be held alongside the reported speeds [29].

For the purposes of this paper the consequences are three. The size is useful: a reported diameter of 1.2 m says the $R = 1$ m placeholder of §7 is the right order. The symmetry is not shared: the official formations number two, four, six or a loose swarm, and none is a rigid 120° triad about an airframe, so, like the Ukrainian corpus above, they enlarge the class and leave the manifold where it was. And the thermal sign is a problem for the plasma reading. A 1.2 m sphere at 1300 mph in sea-level air pays, by Equation 12, on the order of 100 MW in drag. An object dissipating that is not cold. Either the speeds are parallax, which is the conventional reading, or the objects do not exchange momentum with the air, which is the strong claim of §7.5 over again. A self-luminous plasmoid is the one reading the word “cold” excludes. The orbs of Plate I, by contrast, are bright in the thermal cut. If both records are taken at face value they are not the same kind of object.

3. Coordinate frame

Place the airframe mid-body at the origin. The flight axis is $+x$ out the nose, $+y$ along the starboard wing, $+z$ toward the upper vertical tail. A Boeing 777-200ER-class geometry supplies the scale: fuselage length ≈ 64 m, wingspan ≈ 61 m, tail height ≈ 18.5 m. The orbital radius used here, $r = 42$ m, is a modeling choice that keeps the triad outside the wingtip circle and consistent with “orbs not on the skin” in the thermal frames. It is not a photogrammetric measurement. Anyone with calibrated plate scale can replace r without touching the form of the equations.

4. The path

The minimal model is three points equally spaced on a circle that lies in a plane perpendicular to the flight axis and is spun about that axis. For orb $i = 0, 1, 2$:

$$\vec{r}_i(t) = (0,\ r\cos(\omega t + 2\pi i/3),\ r\sin(\omega t + 2\pi i/3)), \quad i = 0, 1, 2$$

Equation 1. Parametric path of orb i about the fuselage axis, in the frame of the airframe.

The phase of each orb is $\varphi_i = \omega t + 2\pi i/3$. Differentiating gives the velocity:

$$\vec{v}_i = r\omega\,(0,\ -\sin\phi_i,\ \cos\phi_i), \quad |\vec{v}_i| = r\omega, \quad \phi_i = \omega t + 2\pi i/3$$

Equation 2. Velocity of each orb; speed is constant at rω.

A single 360° "receiver tune" before vertical lock is one period $T = 2\pi/\omega$. Path length per orb per turn is $2\pi r \approx 264$ m at the scale chosen here. Because x_i is held at the mid-body station, every orbit lies in a plane normal to the flight axis. That is why a single look-angle can make the objects appear to pass in front of, beside, and behind the jet without a large change in slant range. Equations 1–2 are written in the airframe's frame; the path through the air is a helix and is taken up in §7.5.

5. The triangle

At every instant the three positions are the vertices of an equilateral triangle in the *yz*-plane. Side length, area, and angular momentum about the flight axis (each orb treated as mass *m*) are

$$s = r\sqrt{3}, \quad A = \tfrac{3\sqrt{3}}{4} r^2, \quad L_x = 3mr^2\omega$$

Equation 3. Side, area, and axial angular momentum of the rigid triad.

At $r = 42$ m one has $s \approx 72.7$ m and $A \approx 2.29 \times 10^3$ m². The centroid remains on the flight axis for all *t*. That is the geometric meaning of a "metastructure": the triangle is a rigid body in the rotating frame, and any coupling among the three objects — magnetic or otherwise — has L_x as the quantity that can be redistributed if internal spin is torqued into the formation.

If the claimed collapse is real, it is a radial degree of freedom $r(t)$ with $dr/dt < 0$. The triangle remains equilateral while it shrinks until pairwise gaps can no longer support whatever pressure balance is proposed. A collapse trajectory is a one-line extension, $r(t) = r_0 - \alpha t^n$, and should be fitted only against frame-by-frame plate scale. It does not come alone: §7.3 shows that the same L_x fixes what ω must do while *r* falls, and that is the sharpest test in this paper.

6. The torus — the donut envelope

Commentary that the objects "spin around the plane in a donut shape" is a statement about a surface, not a curve. The natural surface is a torus whose major radius is the orbital radius *r* and whose tube radius *a* is the thickness of the luminous sheath or the amplitude of any small radial jitter:

$$x = a\sin v, \quad y = (r + a\cos v)\cos u, \quad z = (r + a\cos v)\sin u$$

Equation 4. Torus of major radius r and tube radius a, axis along x.

A weak axial standing wave — the language of locking vertically, or of a destination on the axis behind the jet — is a small oscillation on x. An earlier draft wrote it as $x_i = A_x \sin \Omega t$ at fixed radius. That curve lies on a cylinder, not on the torus of Equation 4. To ride the torus the axial and radial excursions must move together, with the poloidal angle $v = \Omega t + \delta_i$ and ρ the distance from the flight axis:

$$x_i(t) = a\sin(\Omega t + \delta_i), \quad \rho_i(t) = r + a\cos(\Omega t + \delta_i), \quad a \ll r$$

Equation 5. Axial standing-wave perturbation, written so the path stays on the torus. Each circular orbit becomes a flattened helix.

Three consequences follow. The path closes only if $\Omega/\omega = p/q$ is rational; each orb then traces a (p, q) torus winding — a torus knot when p and q are coprime and both exceed one — and the three orbs together form a three-strand link. A wave that is stationary in the rotating frame, which is what "standing" should mean, requires $\Omega = n\omega$. And the phases matter, more than an earlier revision allowed. With all δ_i equal the three vertices share one poloidal phase: the triangle stays exactly equilateral with side $\sqrt{3}\rho(t)$, every vertex stays on the torus, and the plane breathes along x with its centroid on the axis at $x = a \sin v$. With $\delta_i = 2\pi i/3$ the plane does tilt and precess, but the triangle is no longer equilateral and its centroid leaves the axis: the three ρ_i differ, the side lengths spread by about $a\sqrt{3}$ and the centroid sits $a/2$ off the flight line. Bocker's review [40] identified the error: one expression was being asked to represent two different manifolds. An exact torus winding and a rigid tilted triad are separate branches and must be modelled separately. The rigid branch is written with a rotation matrix:

$$\vec{R}_i(t) = \vec{c}(t) + Q(t)\,\vec{q}_i, \quad \vec{q}_i = r\,(0, \cos\tfrac{2\pi i}{3}, \sin\tfrac{2\pi i}{3}), \quad Q \in SO(3) \;\Rightarrow\; |\vec{R}_i - \vec{R}_j| = \sqrt{3}\,r,\; \tfrac{1}{3}\sum_i \vec{R}_i = \vec{c}$$

Equation 5b. The rigid triad: body-frame vertices q_i carried by a rotation Q(t) SO(3) about a centroid c(t). Equal sides and the centroid are exact for any tilt or precession; the vertices need not lie on one torus.

Equation 5 with a common phase is the toroidal breathing branch; Equation 5b is the rigid tilt and precession branch. The footage can be fitted to either, and the discriminator is the one §8 already asks for: after perspective correction, equal side lengths through a tilt select 5b, while a common axial displacement with the transverse radius obeying the torus relation selects 5. Neither closing within the error model is a non-rigid alternative. A side view distinguishes them.

Figures 1 and 2 render the rigid triad and the perturbed torus at the scale above. The four views in Figure 1 are the same instant. The isometric and along-axis panels make the 120° lock obvious. Top-down collapses the triad toward a line through the mid-body station. The side view shows that every unperturbed path is confined to planes normal to the flight axis.

The May 2025 star in Plate III is a different group. Six lobes at roughly 60° about a single bright core is C_6 symmetry in the plane of the disk, not C_3 symmetry of three separate centers. If those lobes were themselves compact sources on a small circle of radius a, the path would be the same torus equation with $N = 6$ and a much smaller r — a craft-scale hexagram, not an airframe-scale triangle. Nothing in the TYPHOON-HUD file shows three such stars orbiting a jet. The two geometries can live in the same sentence only as members of a class (compact, luminous, multiply-lobed sources under military IR). They are not the same manifold.

Figure 1. Three-orb metastructure about a 777-class airframe · r = 42 m

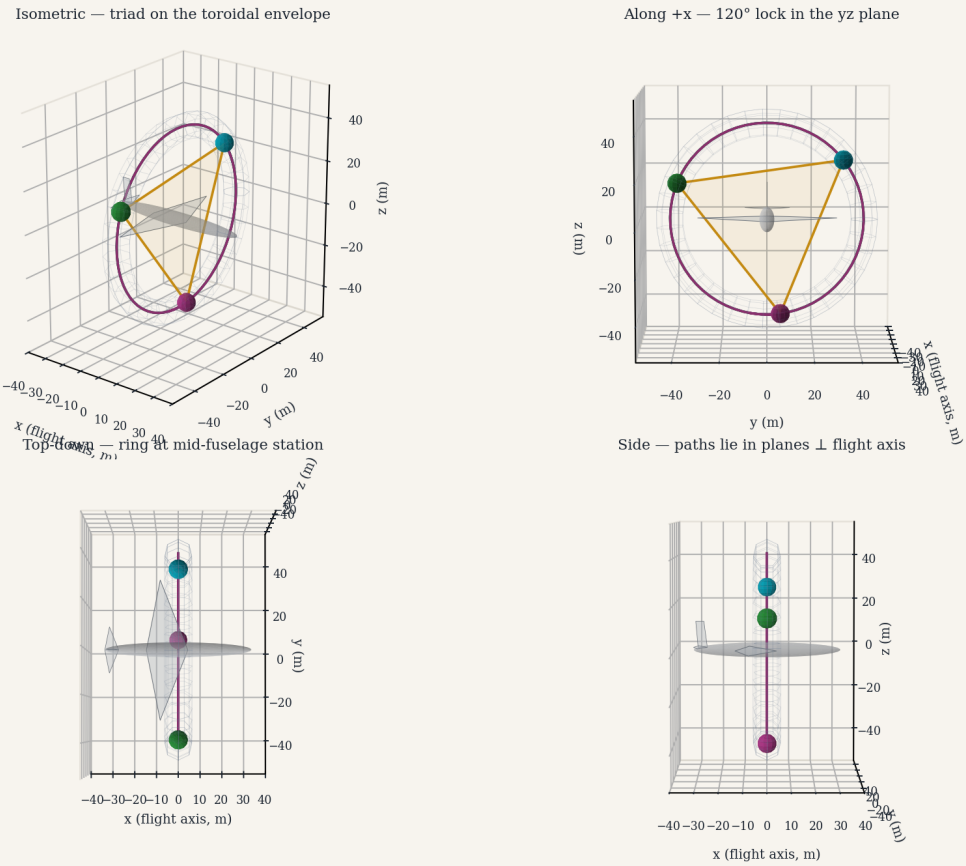


Figure 1. Three-orb metastructure about a 777-class airframe. Orbital radius r = 42 m is a scale choice, not a measurement from the clips.

Figure 2a. yz cross-section of the rigid triad

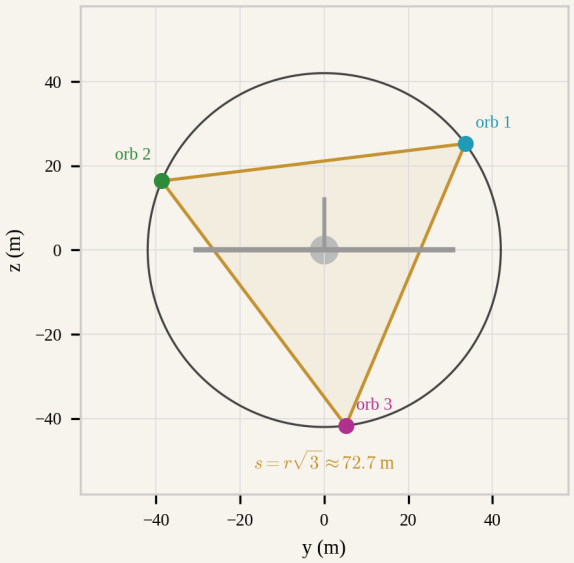


Figure 2b. Torus winding, $\Omega = 3\omega$, $\delta_i = 2\pi i/3$, a = 6 m

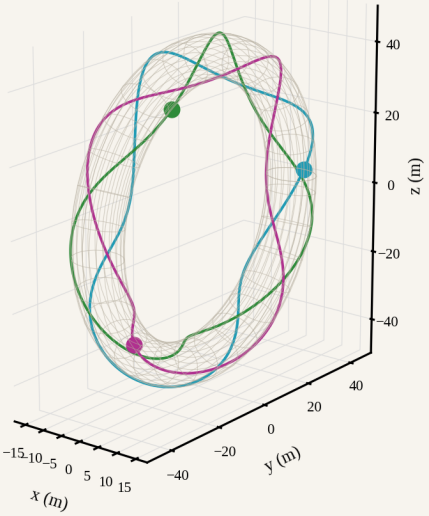


Figure 2. Left: yz cross-section of the rigid 120° triad. Right: the same triad on the torus of Equation 4 with the perturbation of Equation 5 at Ω = 3ω and phases 2πi/3. The tube radius is exaggerated to 6 m so the winding is visible.

7. Dynamics implied by the kinematics

Sections 4–6 say where the objects are. They say nothing about why they stay there. A circle is not a free path: it costs a force, the force has a sign, and the sign and size can be checked against every mechanism proposed for the clips. Numbers in this section assume an orb mass m = 100 kg and radius R = 1 m. Neither is measured. They are placeholders chosen so the scalings can be read, though the 1.2 m diameter logged in the Gulf of Oman file (§2.1) says the radius is of the right order; every result states how it moves with m, R and T.

7.1 The circle costs a force, and the force points inward

Each orb on Equation 1 accelerates toward the flight axis at $r\omega^2$. If the triad is bound by forces between the orbs, the two pair forces on each vertex make 30° with the inward radial, so each pair must *attract* with

$$a_c = r\omega^2 = \frac{4\pi^2 r}{T^2}, \qquad F_{\text{pair}} = \frac{m\, r\omega^2}{\sqrt{3}}$$

Equation 6. Centripetal acceleration of each orb and the attractive pair force that would supply it.

At r = 42 m a four-second rotation is 10.6 g and a two-second rotation is 42 g (Table 1, Figure 3a). That is outside the envelope of any crewed aircraft and inside the envelope of a missile, which is a useful calibration of what is being claimed. More important is the sign. Commentary on the clips, and §9 of this paper, speak of outward magnetic pressure holding the triangle apart. Outward pressure cannot hold a rotating triangle together. Either the net coupling is attractive, or each orb supplies its own inward thrust of $mr\omega^2$ continuously, or the rotation is not mechanical. A reading of the clips has to choose one.

Period T	Orbital speed rω	Centripetal	Speed through air (Mach)	Pair force (100 kg)	Dipole moment M ≥	Surface field (R = 1 m)	Field at fuselage
2 s	132 m/s	42.3 g	283 m/s (0.95)	23.9 kN	10.6×10^8 A·m²	211 T	14 G
4 s	66 m/s	10.6 g	259 m/s (0.87)	6.0 kN	5.3×10^8 A·m²	106 T	7 G
8 s	33 m/s	2.6 g	252 m/s (0.85)	1.5 kN	2.6×10^8 A·m²	53 T	4 G

Table 1. What the circle of Equation 1 costs at r = 42 m, V = 250 m/s, speed of sound 296.5 m/s (ISA, 35,000 ft). Magnetic columns use the most favourable (coaxial) dipole geometry of Equation 10, so they are lower bounds. Moment scales as √m/T; surface field as √m/(T R³).

7.2 A passively bound triad is unstable under any inverse-power attraction

Three bodies at the corners of a rotating equilateral triangle is Lagrange's 1772 solution of the three-body problem. For an inverse-square attraction it is linearly stable only under Routh's condition [20]:

$$\frac{m_1m_2 + m_2m_3 + m_3m_1}{(m_1 + m_2 + m_3)^2} < \frac{1}{27} \qquad (\text{equal masses}: \tfrac{1}{3})$$

Equation 7. Routh's stability condition for the Lagrange equilateral configuration. Equal masses fail it by a factor of nine.

Steeper force laws do not help. Under an attractive central force falling as d^{-n} even a two-body circular orbit is unstable for $n \geq 3$, and the dipole–dipole force falls as d^{-4}. Earnshaw's theorem closes the static case. So a triad bound by any inverse-power attraction and holding 120° through a full rotation is not resting in a potential well. It is being actively held, and a control loop leaves a signature. An earlier revision stated this for every passive binding; Bocker's review [40] showed that is too strong. Routh's result is a theorem about inverse-square attraction, and the power-law argument covers central forces that fall with distance. A binding that stiffens with distance, three

Hooke-like links of stiffness k preloaded to rest length $\ell_0 = \sqrt{3}r - mr\omega^2/(\sqrt{3}k)$, supplies the centripetal force of Equation 6 and tends continuously to the ordinary stable spring triangle as $\omega \to 0$; its rotating equilibrium cannot be excluded by Routh. Passive stability is therefore mechanism-dependent, and the obligation on any proposed binding is the rotating-frame test:

$$U_{\text{eff}} = U - \tfrac{1}{2}\omega^2 \sum_i m_i \rho_i^2, \qquad \nabla U_{\text{eff}} = 0, \qquad \operatorname{Re}\lambda \le 0 \ \ \text{(non-rigid modes)}$$

Equation 7b. Obligation on any passive binding with potential U: an equilibrium of the rotating-frame effective potential, and no exponentially growing mode in its linearised spectrum after the rigid modes are removed.

Inverse-square and dipolar models fail the test; a tether or spring model can pass it. What the clips cannot show is a tether, so for the mechanisms costed in Part II the control-loop conclusion stands, but it stands as a result about those mechanisms, not as a theorem about all of them. If the binding is modelled as three equal springs of stiffness k, the in-plane modes are one breathing mode and one degenerate doublet [21]:

$$\omega_A^2 = \tfrac{3k}{m}, \qquad \omega_E^2 = \tfrac{3k}{2m}, \qquad \omega_A/\omega_E = \sqrt{2}$$

Equation 8. In-plane normal modes of an equal-mass, equal-spring triangle (D3h): breathing mode A and doublet E.

The ratio $\sqrt{2}$ is independent of k and m. Rotation splits the doublet through the Coriolis term, and the splitting scales with ω, so it is a second measurement of the spin. The collapse of §5 is the breathing mode going unstable. A spectrum of the residual jitter in angular spacing and radius, taken from stabilised frames, either shows that structure or shows the smooth interpolation of a keyed path.

7.3 Collapse conserves angular momentum

If the triangle tightens without external torque, $L_x = 3mr^2\omega$ is fixed and Equation 3 forces

$$\omega(t) = \omega_0 \left(\frac{r_0}{r(t)}\right)^2, \quad v \propto r^{-1}, \quad a_c \propto r^{-3}, \quad K = \frac{L_x^2}{6mr^2}$$

Equation 9. Spin-up, and the rotational parts of speed, acceleration and kinetic energy, of the triad during a torque-free collapse.

Equation 9 is exact for the angular rate and gives the rotational components only. A collapse at finite rate has a radial velocity and acceleration of its own, and Bocker's review [40] completed the kinematics. With $h = r^2\omega$ the conserved quantity per unit $3m$, the tangential acceleration cancels identically ($r\dot{\omega} + 2\dot{r}\omega = 0$) and everything else carries an $\dot{r}$ term. The review also generalised the invariant to a rigid triad whose plane is tilted by β from the fuselage normal, using the inertia tensor of three equal masses, $\mathbf{I} = (3/2)mr^2(\mathbf{1} + \mathbf{n}\mathbf{n}^{\mathrm{T}})$ about the centroid:

$$|\vec{v}|^2 = \dot{r}^2 + \tfrac{h^2}{r^2}, \quad \vec{a} = \left(\ddot{r} - \tfrac{h^2}{r^3}\right)\hat{e}_r, \quad K = \tfrac{3m}{2}\left(\dot{r}^2 + \tfrac{h^2}{r^2}\right), \qquad L_x = \tfrac{3}{2}mr^2\dot{\theta}\,(1 + \cos^2\beta)$$

Equation 9b. Full torque-free collapse kinematics, and the axial angular momentum of a rigid triad tilted by β; it reduces to Equation 3 at β = 0 and gives the generalised invariant $r^2\dot{\theta}(1 + \cos^2\beta)$.

Halving the radius quarters the period, multiplies the acceleration by eight and the kinetic energy by four; the attractive coupling must do that work (Figure 3b). This is the sharpest falsifier the clips allow, because it needs no absolute scale: measure ω and the apparent triangle size in the same frames and test whether ωr^2 is constant, or $r^2\dot{\theta}(1 + \cos^2\beta)$ if the plane is tilted, and measure $\dot{r}$ directly rather than inferring the speed from $r\omega$ alone. A collapse at constant ω means an external torque, a non-mechanical object, or an animation; a failure of the material relation

demotes the material-body reading without touching the geometry it shares with the others (§8). There is also a hard geometric limit. At the mid-body station the wing occupies the *xy*-plane out to the 30.5 m semi-span, and each orb crosses that plane twice per turn. The triad cannot shrink below $r \approx 30.5$ m, 73 percent of its starting radius, without striking the wing, unless the plane of the triangle first moves off the wing station along *x*. A side view settles which.

Figure 3a. What the circle costs at r = 42 m

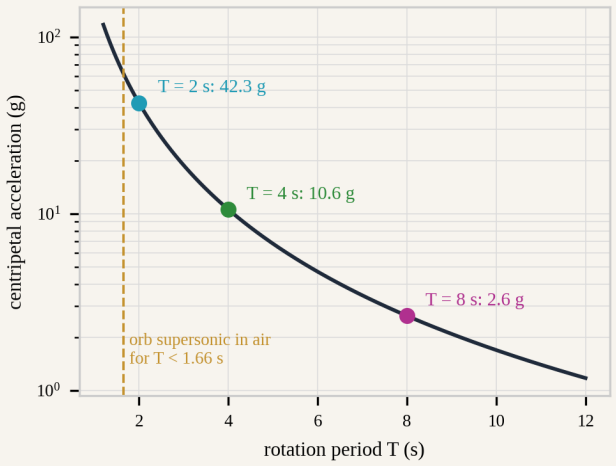


Figure 3b. Collapse at conserved L_x

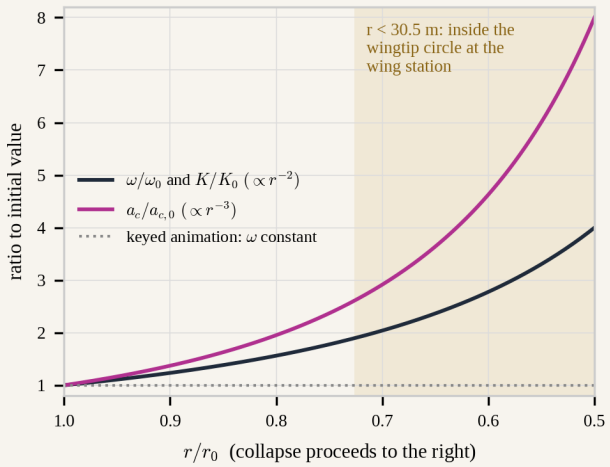


Figure 3. Left: centripetal acceleration on the circle of Equation 1 against rotation period. Right: what Equation 9 requires of a collapse, against the constant-ω path a keyed animation would most naturally follow. The shaded band is forbidden at the wing station.

7.4 A magnetic binding can be bounded

Take the magnetic picture at its word. The strongest attraction two dipoles of moment *M* can exert at separation *s* is the coaxial value, which bounds the moment needed to supply Equation 6 and, through it, the field at the surface of an orb of radius *R* [22]:

$$F_{\max} = \frac{3\mu_0 M^2}{2\pi s^4} \;\Rightarrow\; M \geq \left(\frac{2\pi s^4\, m\, r\omega^2}{3\sqrt{3}\,\mu_0}\right)^{1/2}, \qquad B_{\text{surf}} = \frac{\mu_0 M}{2\pi R^3}$$

Equation 10. Most favourable dipole–dipole attraction, the moment it implies for the triad, and the polar surface field.

For a four-second rotation the moment is 5.3 × 10^8 A·m² and the surface field about 106 T. The strongest continuous laboratory field is about 45 T, and that magnet fills a room. The same dipoles put roughly 7 G on the fuselage, more than ten times the geomagnetic field, which the aircraft's magnetic heading sensors would register. Two geometric facts make matters worse. Three moments parallel to the flight axis, the arrangement the "outward pressure" language describes, repel one another. And three moments cannot all be pairwise coaxial. A head-to-tail ring in the plane of the triangle attracts, but more weakly than the bound. A magnetic binding is therefore not excluded by geometry, but it is excluded by field strength unless the orbs are far lighter than 100 kg or the rotation far slower than the clips suggest.

7.5 The path through the air

In the air the jet translates at $V \approx 250$ m/s and each orb flies a helix:

$$\vec{R}_i(t) = (Vt,\; r\cos\phi_i,\; r\sin\phi_i), \qquad |\dot{\vec{R}}_i| = \sqrt{V^2 + r^2\omega^2}, \qquad \text{pitch} = VT$$

Equation 11. Path of orb i in the air frame, its speed, and the pitch of the helix.

At T = 4 s the pitch is one kilometre, the speed 259 m/s (Mach 0.87), and the velocity is inclined 15° to the flight axis. Below $T \approx 1.66$ s the orbs are supersonic and should drag a shock. The orbit plane sits at mid-body, ahead of where the contrail forms, so the orbs do not cut the contrail itself; an earlier note of mine to that effect was wrong. What they must do, if they are bodies that exchange momentum with the air, is leave three helical wakes of pitch VT wrapped around the contrail at radius r. The jet is drawing a contrail in Plate II E, so the air is cold and moist enough to show one, and a transonic metre-class body in such air leaves a thermal wake and often an aerodynamic condensation trail of its own [25]. No wake means no momentum exchange, which is a strong physical claim, or no body.

7.6 Power: radiated and aerodynamic

Two budgets can be read off a calibrated thermal frame:

$$P_{\mathrm{rad}} = 4\pi R^2\,\varepsilon\sigma T_s^4, \qquad P_{\mathrm{drag}} = \tfrac{1}{2}\rho\, C_D\, \pi R^2\, |\dot{\vec{R}}|^3$$

Equation 12. Grey-body radiated power of an orb at surface temperature Ts, and the power needed to push it through the air.

For R = 1 m a 1000 K surface radiates about 0.7 MW and a 2000 K surface about 11 MW. The sources in Plate I are unresolved, so a radiometric calibration gives the product $\varepsilon R^2 T_s^4$ rather than each factor, but that product is exactly what a power estimate needs. Drag at $C_D \approx 0.5$ and air density 0.38 kg/m³ costs about 5 MW per orb for as long as the formation holds. If the luminous object is a plasma at the ambient 0.24 atm, recombination runs at $\tau \approx 1/(\alpha n_e)$ with α of order 10^{-13} m³/s for molecular ions: 10^{-5} to 10^{-7} s for electron densities of 10^{18} to 10^{20} m^{-3}. Laboratory FRCs live for milliseconds in vacuum. A plasmoid that glows for minutes in the open stratosphere is being fed continuously, at megawatts, from a metre-scale volume, with no visible reaction mass. That is the real size of the claim, and it is better stated than implied.

7.7 Dimensionality and scale

Every result in §§4–7 was derived in a plane, and several of the comparisons in Part II carry a laboratory quantity across many orders of magnitude in size. Norbert Schwarzer, reviewing an earlier revision, warned that neither is bookkeeping: it matters whether a flow is restricted to two dimensions, allowed three, or, in his phrase, “three-plus”, with parameter dependencies entering the equations; and results carry scale dependences that are easy to lose. This subsection records which claims are dimension-sensitive, which cross scales, and one formulation, his, in which both dependences are explicit.

The circle of Equation 1, the pair force of Equation 6, Routh’s condition and the modes of Equation 8 are two-dimensional statements. Out of the plane an equal-spring triangle has three further modes, two rigid tilts and an umbrella, and it is the tilt rather than the breathing mode that the plasmoid analogy of §9 should fear: the fastest-growing instability of a laboratory FRC is the n = 1 tilt, invisible in any axisymmetric or planar calculation and found only when the third dimension is admitted [2]. The same is true of the fluid. An orb of metre radius at Mach 0.87 in stratospheric air has a Reynolds number of order 10^7 (about 1.4×10^7 for R = 1 m); its wake is three-dimensional and turbulent, and two- and three-dimensional turbulence behave in opposite ways. In two dimensions energy cascades toward large scales and coherent vortices persist; in three dimensions vortex stretching cascades it toward small scales and organised structures are torn apart. A planar model therefore flatters the triad twice. It hides the tilt mode, and it hides the mechanism by which a real atmosphere destroys organised flow. The stability arguments of §7.2 are necessary conditions. They are not sufficient until the tilt is included, and the side view that §7.3 and §11.4 already ask for is the observation that constrains it.

Scale enters in three places, each of which compares a laboratory quantity with an object metres across. Section 11.4 sets a Casimir energy density at 10 nm against the negative energy of a 30 m throat, seventeen orders of magnitude apart in length, and the arithmetic assumes the quantity is the same kind of thing at both scales. Section 13 carries centimetre fireballs fed with kilowatts to metre orbs fed with megawatts, and the scaling is unfavourable: surface losses grow as R^2, the volume to be sustained as R^3, and no published fireball has crossed a decimetre. Section 12 carries a pinch of centimetre radius and a hundred nanoseconds to a sphere of a metre and minutes, and the codes named there include two-dimensional ones; the kink that limits every pinch is a three-dimensional event, and only a three-dimensional result counts for it. Table 2 collects the entries.

Claim	Derived in	Sensitive to	What would settle it
Circle and pair force (Eq. 1, 6)	Plane	Nothing new; exact for a rigid triad	—
Routh condition, spring modes (Eq. 7, 7b, 8)	Plane	Out-of-plane tilt and umbrella modes; mechanism of binding	Side view; rigid tilt of Equation 5b
Magnetic binding bound (Eq. 10)	Three-dimensional dipoles	None	—
Drag and radiated power (Eq. 12)	Three dimensions, empirical C_D	$\mathrm{Re} \approx 10^7$ wake; a 2-D estimate cannot be used	Radiometric calibration of the thermal frames
Plasmoid analogy (§9, §12)	Laboratory, centimetres, vacuum	$n = 1$ tilt and kink (3-D); four to six orders in size and time	Three-dimensional simulation; flicker test of §12.5
Negative-energy comparison (§11.4)	General relativity at 30 m against QED at 10 nm	Whether the comparison is scale-free	Recomputation with a scale factor carried through
Buoyant shell (§13)	Centimetre fireballs	R^2 losses against R^3 volume	Bench test of §16.2

Table 2. Which claims of this paper depend on the dimension in which they were derived or on the scale across which they are compared, and what would settle each. Entries marked — are not at risk.

One formulation makes both dependences explicit rather than implicit, and since it is the source of the warning it is recorded here as a possibility. Schwarzer [39] works from a scaled metric, $G_{\alpha\beta} = F[f]\cdot g_{\alpha\beta}$, inserted into the Einstein–Hilbert action, and shows that the quantum equations then follow from the same variation that gives gravity. Three features bear on this paper. The number of dimensions n appears as a coefficient in the resulting field equations, not as a background assumption: the term nonlinear in the gradient of f grows with n while the curvature terms recede, which is his account of why gravity is weak, and a result derived in a fixed low-dimensional setting does not carry over when parameter dimensions are added — his “3D+”. The scale factor $F[f]$ is a choice, of the form $(C_f + f)^{4/(n-2)}$ in the cases he works through, and the physics recovered depends on it, so a quantity such as a vacuum energy density is not scale-free, and a comparison across seventeen orders of magnitude is not guaranteed to be a comparison of like with like. And the action is not taken to be exactly stationary but to sit a parameter off its extremum, what he calls the ever-jittering fulcrum, so that a residual jitter about an equilibrium is expected rather than incidental. He also finds that bounded coherent regions of the scaled field radiate by their nature, with spherical wave solutions of Klein–Gordon type around them.

If that formulation is right, three things in this paper change and one does not. The energy comparison of §11.4 becomes a comparison across scale regimes, and its conclusion, hopeless by seventeen orders of magnitude, would have to be recomputed with the scale factor carried through. This paper does not do that, and does not claim the result would come out favourably; it says only that the present arithmetic assumes what his framework denies. The residual jitter in spacing and radius that §7.2 proposes to measure becomes a quantity with structure of its own rather than a nuisance, though the measurement is the same. And a self-luminous sphere acquires a third reading beside the plasmoid and the fusion core: a coherent domain that radiates because it is bounded, with no reaction

inside it at all. The single-band thermal frames cannot separate that from a hot plasma; a spectrum might, since the two need not share a grey-body form. What does not change is the geometry. The circle, the triangle, the torus and the collapse rule are measurements of a path, and they stand or fall on the footage whatever metric underlies it. The paper takes no position on the framework. It records it because it is the only formulation on the table in which the two warnings, dimension and scale, are consequences of the equations rather than cautions attached to them, and because the review that raised them is the review this paper asked for. The author thanks Norbert Schwarzer for the comments that prompted this subsection; any misstatement of his work is the author's.

8. What would confirm or break the model

A model earns its keep by naming the measurement that would kill it. Four tests are geometric:

- **Stereo disparity.** If the circulating files contain two independent views, matching points on airframe, clouds, and each orb must obey one fundamental matrix. A single consistent depth hierarchy — nearby cloud tops shifting more than distant layers, each orb occupying a distinct depth surface — would support a real volume. A uniform horizontal shift would support a duplicated 2-D plate.
- **Angular spacing.** After perspective correction, the three sources should remain near 120° in the plane normal to the fuselage through the locked phase. Systematic drift away from 120° breaks rigidity.
- **Occlusion order.** Front-to-back passages of each orb against the tail and wing must agree with the rotating-triad depth order, not with a flat overlay.
- **Period.** The locked spin should be a single well-defined ω. A changing period that cannot be explained by look-angle, platform motion, or Equation 9 is either a different manifold or an artifact.

Seven more follow from §7, §11.4 and §14 and need no new footage:

- **Spin-up.** Through any tightening, ωr^2 should be constant (Equation 9), or $r^2\dot{\theta}(1 + \cos^2\beta)$ if the plane tilts (Equation 9b), with $\dot{r}$ measured rather than inferred. Both quantities are image-plane measurements in the same frames, so no absolute scale is required. The test binds the material-body reading only.
- **Mode structure.** Residual jitter of a held formation should show a breathing line and a doublet near $1/\sqrt{2}$ of it, the doublet split in proportion to ω (Equation 8). Smooth interpolation shows neither.
- **Wing clearance.** The triangle cannot pass inside the wingtip circle at the wing station. A side view must show the plane of the triad moving along x before r falls below the semi-span.
- **Wakes.** Three helical trails of pitch VT about the contrail, or a stated reason why a transonic body leaves none.
- **Pointing.** If a fourth source at the destination is taken seriously (§11.4), the locked triad's plane must tilt from the fuselage normal by half the great-circle angle to that destination. An untilted plane names no place on Earth.
- **Shadow and flicker.** If the sources are foci of projected energy rather than bodies (§14.2), each must vanish in the sector where the airframe blocks its beam, and must flicker at the source's pulse rate. Neither is expected of a body or of an overlay.
- **Radiometry.** In-band radiant intensity of each source, converted through Equation 12 to a power, compared with the drag power at the measured speed. The two should be commensurate for any thermal source.

Bocker's review [40] adds the structure these tests sit in, and it is adopted here. Three unconstrained points are nine coordinates; a single view supplies six, so the positional null space of one camera has dimension three and no amount of fitting removes it. Two genuinely independent calibrated views close it. But closing the geometry does not identify the generator: with three further coordinates standing for the mechanism class, material body, field-defined focus, or image-plane composite, stereo still leaves a null space of three, and only

mechanism-sensitive channels, the wake, flicker, shadow, radiometry and compositing tests above, can close it. The hierarchy is observations → general threefold geometry → {toroidal breathing, rigid tilt, collapse} → {body, focus, composite}, with three promotion rules: a projection fit does not imply a unique three-dimensional geometry; a unique geometry does not imply a generator; and mathematical admissibility is not physical establishment. A failure in one generator class is never a failure of the geometry the classes share.

Until those tests are run on original files, the reconstruction remains a hypothesis about shape. That is still useful. A wrong manifold wastes years. A right one tells an experimentalist where to point a sensor.

PART II

Candidates, mechanisms and open questions

Each proposed mechanism stated, separated into what is established and what is not, and costed against Part I.

9. Adjacent laboratory geometries (with the Lockheed compact fusion program)
10. The Pais Effect and the Navy filings
11. A candidate core — the spherical IEC
12. A second candidate — the pulsed Z-pinch
13. A third candidate — the buoyant plasmoid
14. Steering — fields, software and intention
15. Separating the mouths — distance and time
16. A programme to close the gaps
17. Closing

9. Adjacent laboratory geometries — analogy only

Self-organized luminous spheres are not unknown in the laboratory. Field-reversed configuration plasmoids confine plasma in a compact, largely self-contained magnetic structure without a set of external toroidal coils. Polyhedral (Polywell-type) cusp arrangements place magnetic mirrors at the vertices of a regular polyhedron and have been studied as a route to high-β confinement. Neither device teleports an airframe. Both do produce compact, roughly spherical, magnetically dominated objects that can be moved as a formation. A closer topological cousin, taken up in §11, is the spherical inertial-electrostatic confinement (IEC) device: a ported anode shell with a transparent cathode grid and a dense, non-Maxwellian core.

The reason they belong in a footnote of this paper is architectural, not evidentiary. A three-body force-free arrangement is a natural first guess if one is already thinking in plasmoids. Overlapping dipole-like fields at 120° give a simple picture of "outward magnetic pressure holding the triangle apart," and reconnection at the mid-plane of each pair is the ordinary way those fields would reconfigure if the balance failed. That sentence is a dictionary between the commentary on the clips and the vocabulary of laboratory plasma. It is not a conclusion that an FRC was flying in 2014.

Section 7 sharpens the dictionary and removes part of it. "Force-free" is a statement about $\mathbf{j} \times \mathbf{B}$ inside one plasmoid. It is not a statement that a formation of plasmoids needs no force. Parallel moments do repel, which is the outward-pressure picture, but a rotating triad needs a net inward force on every vertex (Equation 6), so outward pressure alone flies apart. The plasmoid reading therefore needs a second, attractive agent, and Equation 10 says a magnetic one would have to exceed laboratory fields. The analogy survives as morphology. It does not survive as mechanics without an addition nobody has yet named. It also inherits the three-dimensional instabilities of the laboratory object, which §7.7 takes up: a planar picture of three plasmoids at 120° has no room for the tilt mode that limits a real FRC.

The author's own work sits in aneutronic plasma and dual-use compact sources. That is disclosed so the reader can discount enthusiasm where it appears. Enthusiasm is not a substitute for stereo.

9.1 A named program: Lockheed Martin's Compact Fusion Reactor

Commentary on the clips does not stop at a class of device. It points to a program: the Compact Fusion Reactor (CFR) at Lockheed Martin's Skunk Works. The public trail it cites is real. Charles Chase presented the effort at Google's Solve for X on 7 February 2013; *Aviation Week* was given access to the laboratory and published the concept in October 2014 with Thomas McGuire as technical lead; experiments labelled T4 and T4B were reported, and in July 2019 Skunk Works said a larger T5 was under construction. After that the program went quiet. It is cited here as a possibility the commentary raises, and the record should be stated exactly, because two parts of the usual telling need correcting [26].

First, the silence did end. On 28 August 2023 a Skunk Works executive confirmed that the CFR had been cancelled at least three years earlier, after a team of about 25 had worked through 2019, so that the company could concentrate on core technology. That is a public statement of termination. It is not a technical post-mortem, and those who read the quiet years as a program going dark rather than ending will note that the two look alike from outside. A reader should still know the statement exists.

Second, the published CFR is not the device the commentary describes. In that reading the glowing spheres are field-reversed configuration plasmoids or compact reactors, high-β, aneutronic, burning proton–boron-11. The CFR of the patents and presentations is high-β, but it is a magnetic cusp and mirror machine with superconducting coils

inside the plasma, it carries no net plasma current, and it was designed for deuterium–tritium with a lithium blanket. T4B was a vessel about 1 m by 2 m, heated at 1 MW for 3 ms, reporting ion temperatures near 75 eV; the power-plant concept grew to roughly 7 m by 18 m and 2000 tonnes. None of that is a free-flying metre-scale sphere. The published program that does match "FRC, high-β, p–^{11}B" is TAE Technologies', whose machines are tens of metres long [27].

Fuel matters for the geometry. §7.6 asks each vertex for megawatts. A D–T source delivers four-fifths of its power as 14 MeV neutrons: 10 MW is 3.5×10^{18} neutrons per second, or about 1.6×10^{10} per cm² per second at the fuselage 42 m away, unshielded — a lethal dose in well under a minute, and an activation signature in any recovered debris. The aneutronic reading avoids that, at a price: p–^{11}B wants ion temperatures above 100 keV, three orders beyond what T4B reported, and in a thermal plasma its bremsstrahlung loss exceeds its fusion power, which is why the published attempts rely on non-thermal, beam-driven cores of the kind taken up in §11. So the CFR citation is best held as follows: a real, well-funded compact-fusion effort existed at the right company in the right years, and that is all the public record supports. It does not supply the sphere, the fuel, or the flight.

Plate IV is included at this point because the commentary that names the Skunk Works program also circulates photographs of wingless elongated objects as its possible products. This one was supplied to the author. It was taken in Florida by a photographer who has asked not to be named; the date, camera, focal length and range have not been disclosed, and no original file has been examined. The frame is a heavy enlargement. It shows a dark, smooth, elongated form with an aspect ratio of about five to one against clear sky, with no visible wings, tail or plume at this resolution. The thin bright rim is characteristic of sharpening and compression around a dark edge; it sits only slightly above the sky brightness and should not be read as a glow. Nothing in the image establishes size, distance or speed, and nothing connects it to Lockheed Martin or to any program. It is reproduced as an example of the class of report, in the same spirit as Plates I–III: a shape to be measured if better data arrive, not evidence of what made it.



Plate IV. Elongated object photographed in Florida; photographer undisclosed at their request. Enlarged crop supplied to the author; date, equipment and range not disclosed, original file not examined. Bright rim is a sharpening artifact. No connection to any named program is established.

Plate V is a different kind of image and is labelled accordingly. It circulates with the same commentary and shows a white, wingless, capsule-shaped fuselage in a hangar. It is not a photograph. It has the marks of a computer-generated picture: a flag whose stars do not form the real pattern, a row of windows that shrink and crowd irregularly toward the tail, markings that resolve into no letters, and undercarriage that does not match from one leg to the next. It is reproduced, with that label carried inside the frame, for one reason only. It is an accurate picture of what people *mean* by the Tic-Tac of §12.1: the smooth oblong hull, the absence of wings, tail and intakes, the proportions of roughly five to one that Plate IV also shows. It depicts no vehicle that is known to exist, and it has no

connection to Lockheed Martin or to any facility.



Plate V. Concept illustration of a wingless capsule-shaped vehicle, computer-generated; source unknown. Not a photograph, not a depiction of any real vehicle, hangar or program. Included to show the form under discussion.

The same commentary frames propulsion and the vanishing flash not as rocketry but as magnetohydrodynamic and vacuum-energy effects: the dynamical Casimir effect, negative-energy pressure, a wormhole or macroscopic tunnelling. The MHD part is ordinary physics and falls under §7.5: a $\mathbf{j} \times \mathbf{B}$ thruster in ionised air pushes on the air, so it leaves a wake and pays the drag bill of Equation 12. The vacuum-energy part is sized in §11.4.

10. The Pais Effect and the Navy filings

Salvatore Cezar Pais, then an aerospace engineer at the Naval Air Warfare Center Aircraft Division (NAWCAD / NAVAIR, NAS Patuxent River), is the inventor on a cluster of U.S. Navy filings from 2016–2019. In interviews with Ashton Forbes, Dave Rossi, and Jesse Michels he has said the circulating orb sequences display the phenomenon he named the Pais Effect — in one telling, a bubble of non-ionizing radiation forming around the airframe; in another, the terminal flash as a singularity. Those statements are interpretations of pictures. They are not measurements. They do, however, name the only published Navy-assigned mechanism that is built from the same verbs as the clips: charged matter, accelerated spin, a circumferential field, a conditioned vacuum.

10.1 What Pais wrote

The Effect, in Pais's own phrasing, is "the controlled motion of electrically charged matter (from solid to plasma) via accelerated spin and/or accelerated vibration under rapid (yet smooth) acceleration–deceleration–acceleration transients." The claimed consequence is an electromagnetic energy density high enough to couple to the local vacuum state and, in the inertial-mass patent, to polarize that vacuum so that a craft's resistance to acceleration falls. The high-energy electromagnetic field generator (HEEMFG) is the machine that is supposed to produce the Effect; the craft patent puts a vibrating, microwave-driven resonant cavity around a hull; the plasma compression fusion device (PCFD) puts the same spin-and-vibration idea into a pair of counter-spinning charged "dynamic fusors."

A 2019 paper in *IEEE Transactions on Plasma Science* restates the PCFD as counter-spinning electrically charged cones inside a cross-duct, compressing fuel into a high-power-density plasma burn. That paper is the only peer-reviewed item in the cluster. It describes a reactor concept. It does not report a measured Effect.

Filing	Number	Granted	Status
Craft using an inertial mass reduction device	US 10,144,532 B2	4 Dec 2018	Expired (fees unpaid)
Electromagnetic field generator (HEEMFG)	US 10,135,366 B2	20 Nov 2018	Expired (fees unpaid)
High frequency gravitational wave generator	US 10,322,827 B2	18 Jun 2019	Expired (fees unpaid)
Piezoelectricity-induced room-temperature superconductor	US 2019/0058105 A1	—	Abandoned
Plasma compression fusion device	US 2019/0295733 A1	—	Abandoned

Table 3. Navy-assigned Pais filings, 2016–2019. Three grants followed a letter from Dr. James Sheehy (CTO, Naval Aviation Enterprise) to the USPTO stating the inventions were operable and citing foreign competition. All three grants later lapsed.

10.2 What was tested

NAWCAD has said on the record that it tested the Pais Effect from October 2016 to September 2019 at a cost of about $508,000, most of it salaries, and that “the Pais Effect could not be proven.” That sentence is the official experimental result. It does not say the Effect is impossible; it says the test as run did not produce it. Pais has later told interviewers the article under test was not built to his specification. A reader can hold both facts at once: the Navy spent real money, and the Navy did not publish a positive result.

10.3 What Pais said about the clips

In the Forbes / Rossi conversations Pais describes watching an orb begin to circle the airframe, then a second, then a third, and recognizing in advance — on his account — that a “bubble” would form and that a terminal event would follow. He has called that event the Pais Effect made visible. In the Michels conversation he is reported as reading the terminal flash as a singularity and as saying a fourth source is required if a destination is being selected — and, on his account, that the fourth source was not with the other three at all but at the destination, on the far side of the throat. Those are the claims. They are not accompanied by plate scale, a field estimate, or a frequency.

The geometric overlap with §§4–6 is real and limited. Pais’s verbs are spin, vibration, and a high-frequency electromagnetic sheath around a hull. The triad model is three compact sources spinning about a hull on a torus. If one grants his mechanism, the torus in Equation 4 is the sheath, ω in Equation 1 is the spin he requires, and the claimed vacuum polarization would sit in the tube of that torus. That is a dictionary, not a demonstration. Nothing in US 10,144,532 B2 predicts three discrete luminous vertices rather than a continuous glowing hull. Nothing in the IEEE paper predicts a 120° lock. The fourth-orb remark needs care. Read as four sources about the airframe it would be contradicted by Plate I, which shows three. Read as Pais intends it, with the fourth at the destination, it is consistent with three in frame — and for the same reason it cannot be tested on these clips at all, since the object that would confirm it is by construction outside every frame. §11.4 draws out the one consequence of that reading that *is* visible from the departure end.

Two further cautions. A granted patent is a legal instrument, not a working device; the USPTO does not reproduce the physics. And an inventor recognizing his own sketch in a video is the least surprising event in this literature. The useful residue is the short list of quantities his filings actually name — rotation rate, vibration band (he writes 10^{9}–10^{18} Hz), energy density, and a polarized near-field vacuum — any one of which could be asked of a calibrated

frame. Until those numbers are measured, the Pais reading remains a commentary on the pictures, not a confirmation of the patents.

10.4 The scale a conditioned vacuum would need

“Polarizing the vacuum” has a definite meaning in quantum electrodynamics and a definite threshold. The vacuum responds nonlinearly as the field approaches the Schwinger value [24]:

$$E_S = \frac{m_e^2 c^3}{e\hbar} \approx 1.3 \times 10^{18}\ \mathrm{V/m}, \qquad u_S = \tfrac{1}{2}\varepsilon_0 E_S^2 \approx 8 \times 10^{24}\ \mathrm{J/m^3}$$

Equation 13. The Schwinger critical field and the energy density it corresponds to.

A 100 T field, already beyond §7.4, stores about 4×10^9 J/m³: fifteen orders of magnitude short. Below threshold QED does predict small effects, such as a vacuum birefringence of about 4×10^{-24} per tesla squared, and those are being searched for with optical cavities. None of them alters inertia. A claim that a microwave-dressed hull conditions the vacuum is a claim that fifteen orders have been found somewhere. The filings do not say where.

11. A candidate core — suggestion only

Nothing in §§4–6 requires a particular power plant. The path is kinematics. If one still wants a laboratory object that could sit at each vertex of the triad, and that could also account for the six-lobe star in Plate III, the published machine that shares the most topology is the spherical inertial-electrostatic confinement device developed by George H. Miley and collaborators at the University of Illinois. This section is a suggestion. It is not an identification of the objects in the clips.

11.1 George H. Miley

George Hunter Miley (b. 1933, Shreveport) is professor emeritus of nuclear, plasma and radiological engineering, and of electrical and computer engineering, at the University of Illinois at Urbana–Champaign. He took a B.S. from Carnegie Mellon (1955) and an M.S. and Ph.D. in nuclear/chemical engineering from Michigan (1956, 1959), spent two years at GE’s Knolls Atomic Power Laboratory, and joined Illinois in 1961. He directed the Fusion Studies Laboratory from 1975 and chaired the nuclear engineering program. He is a fellow of the ANS, APS, and IEEE; a Guggenheim Fellow; and a recipient of the Edward Teller Medal (1995), the IEEE Nuclear and Plasma Sciences Award in Fusion Technology (2003), and the ANS Radiation Science and Technology Award (2004). He was founding editor of *Fusion Science and Technology*.

The work that matters for this paper is the compact, advanced-fuel line. In the 1970s Miley argued that D–^{3}He and p–^{11}B were not curiosities: they cut neutron damage and open direct conversion. In the 1990s he revived inertial-electrostatic confinement as a small spherical machine that could attempt those fuels because its core is non-Maxwellian and beam-dominated rather than a thermal tokamak plasma. The Urbana devices — ported stainless spheres with a transparent inner grid — are the laboratory objects in that line. NPL Associates, which he founded, has been the industrial counterpart. Colleagues have called him the father of advanced-fuel fusion; the phrase is honorific, not a claim that breakeven was reached. What was reached, and published, is a family of compact spheres that run star mode and jet mode and that were designed, from the start, to burn charged products.

11.2 What an IEC sphere already is

An IEC is a grounded spherical anode with a highly transparent cathode grid inside it. Ions fall toward the center, pass through, climb out, and fall again. At sufficient current the space charge writes nested electrostatic wells — a virtual cathode inside a virtual anode. Miley's program was explicit that this non-Maxwellian, beam-beam core is one of the few compact geometries that can attempt aneutronic fuels (p–^{11}B, D–^{3}He) rather than D–T. The products of those reactions are charged. That matters only if one is already thinking about coupling one sphere to another, or about emptying a well along a chosen axis.

Two documented operating modes of the same vessel rhyme with the two silhouettes in the plates, and that is the whole of the suggestion.

Star mode. Ions do not fill the volume. They run in discrete microchannels that thread opposite grid openings and cross at the center. On a thermal or night-vision plate that would look like a bright core with *N* radial lobes. Six running openings would be a six-fold star. Plate III B is that shape. The rhyme is morphological. It is not a measurement of a grid.

Jet mode. Open one port and the well becomes asymmetric. A collimated plasma column leaves through the hole. Miley and coworkers patented this as a thruster (US 6,121,569): fusion products and residual plasma as a directed jet, with optional collector grids for direct conversion. Plate III's warm axial plume is the same silhouette. Again, a rhyme — a sphere that can grow a plume when one channel is favored.

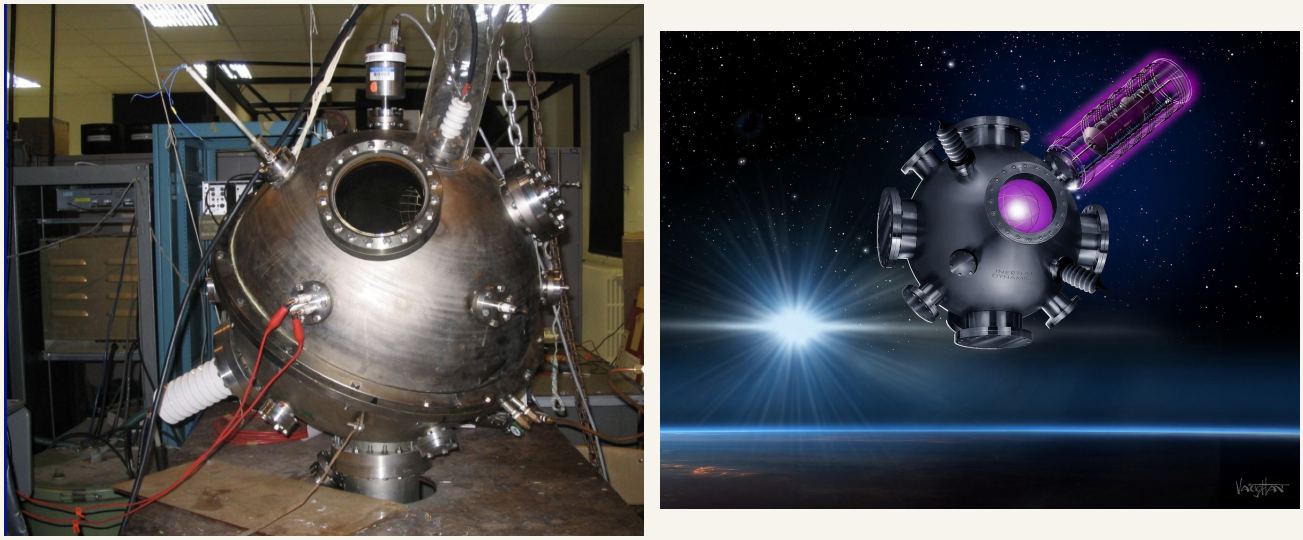


Figure 4. Left: a ported spherical IEC vacuum vessel in the laboratory — anode shell, diagnostic and high-voltage flanges, the geometry of star and jet modes. Right: artist's conception (signed Vaughan; marked Inertial Dynamics) of the same class of object in a flight configuration, core well lit, one port promoted to a jet. Neither image is a frame from the circulating clips. They are included so the reader can see the hardware the suggestion is about.

11.3 Three spheres, if one grants the formation

A single IEC, however well it matches a star, is not the triad. The suggestion is only that three such spheres, small enough to sit at the vertices of Equation 1, could be the compact sources in Plate I. Phase-locking the inward-pointing microchannels would put three virtual cathodes on a circle about the fuselage, with the formation null on the flight axis — the same axis already used for the standing-wave antinode in Equation 5.

Aneutronic yield would, in that picture, be a coupling fluid rather than a headline. Alphas leaving one well can be seed ions for the next. The triangle becomes a circuit. That is possible on paper. It has not been run as a three-body

lock in any published IEC campaign. Section 7 adds the bill. Laboratory IECs run at kilowatts and have never approached breakeven, while §7.6 asks each vertex for megawatts; and a beam of charged products crossing 73 m of air at 0.24 atm is stopped within tens of centimetres, so the circuit would have to be closed by fields, not particles.

The Pais stack from §10 would sit, if it sits anywhere, on the *outside* of each anode shell: a charged, vibrated, microwave-dressed surface whose Poynting flux occupies the torus tube of Equation 4. Whispering-gallery resonators in that shell would be a laboratory way to hold the circumferential standing wave. The IEC would remain the core that holds the well. The HEEMFG would remain a claimed dressing of the vacuum around that well. Neither claim is needed to write the path. Both are optional readings of how a vertex might be built.

11.4 What a “portal mode” would have to be, if it were anything

Commentary on the clips treats the terminal flash as a throat. Under known electrodynamics a classical Maxwell field cannot supply the negative energy a general-relativistic shortcut requires. The requirement can be given a size. A traversable Morris–Thorne throat of radius r_0 needs negative energy of order [23]

$$|E_-| \sim \frac{r_0 c^4}{G}, \qquad \hat{\alpha} \simeq \frac{4G|M|}{c^2 b}$$

Equation 14. Negative energy scale of a traversable throat of radius r0, and the light deflection produced by any mass-energy |M| at impact parameter b.

For a throat wide enough to pass a 61 m wingspan, r_0 = 30.5 m, that is 3.7×10^{45} J: the rest energy of 21.6 Jupiters, with a minus sign, at c^2/GM_J = 0.709 Jupiter masses per metre of throat *radius*. This is not fringe arithmetic. The same expression is Equation 9 of the Defense Intelligence Reference Document “Traversable Wormholes, Stargates, and Negative Energy” (6 April 2010), commissioned under the AAWSAP program and published in the sixth PURSUE release, which gives −0.71 Jupiter masses per metre and labels its length “a suitable measure of the linear dimension (width or diameter) of the throat” [30]. An earlier revision of this paper took that label literally and multiplied by the 61 m opening to get −43 Jupiter masses, a factor of two above the first figure; Bocker’s review [40] caught the inconsistency. The coefficient is c^2/GM_J per metre of radius, as Equation 14 is written, and the benchmark is the radius figure. It is a benchmark tied to the Morris–Thorne metric class, not a lower bound over every traversable construction, and the weak-field deflection in Equation 14 is a scale, not a controlled prediction, once the gravitational parameter is of order one. The document is careful on two points that cut in opposite directions, and both should be reported. It calls that figure a gross upper limit, citing the result of Visser and co-workers that wormhole geometries exist which are supported by arbitrarily small total amounts of negative energy, and it argues that the quantum inequalities — which most of the field takes to confine negative energy to very small scales and durations [23] — are unproven in curved four-dimensional spacetime. It also finds every known laboratory source hopeless at this scale. A Casimir-supported throat needs a plate spacing $d = 4.05 \times 10^{-18}$ $\sqrt{r_0}$ metres, which for r_0 = 30 m is 2×10^{-17} m, far smaller than a nucleus; the scheme is set aside. The moving-mirror, or dynamical Casimir, flux is called exceedingly small and is set aside as well. And classical electric and magnetic fields, however intense, present a non-negative energy density to every observer. The government’s own study leaves the door open in theory and finds no mechanism in hardware.

The same document says what a throat would look like, and for a paper about pictures that is more useful than the energy. A spherical Morris–Thorne mouth deflects light passing through and around it and appears as a sphere holding a shrunken, distorted image of the far region, like a mirrored ornament. A flat-faced “stargate” would show the far region undistorted. A small mouth opening into local space would appear as an unusually bright spot,

blue-shifted while it grows and red-shifted while it recedes. Equation 14 also gives the deflection such a mass-energy would produce if it acted as a simple lens: more than a radian at 100 m. Two qualifications from the document apply. It notes that the equivalent mass of Equation 9 is not the mass seen from far away, which can be zero, so a far-field deflection bound says little; and the flat-faced case does not lens at all. What survives is the near field and the image. Light passing within a throat width of a spherical mouth, which here means the clouds seen just around the aircraft, should be visibly displaced; and in either geometry the opening should show the destination — another sky, another cloud deck, ground — rather than a symmetric ring of light. The flash frames were not examined for this paper. As generally described, including in the comparison of §1.1, they show a radially symmetric burst over an undisturbed cloud field, with no image of anywhere else; that should be checked on the best copies. The thermal cut is a single band, so the predicted blue-then-red asymmetry cannot be tested on it. On that description the strong reading is not supported by the frames, and it is not needed by anything else in this paper.

The vacuum-energy mechanisms named in §9.1 can be put on the same scale. The dynamical Casimir effect is real: a boundary condition modulated at gigahertz rates in a superconducting circuit converts vacuum fluctuations into pairs of microwave photons, at minute powers. An accelerating mirror does in principle emit a negative energy flux, but at a level the reference document itself declines to pursue. The static Casimir effect gives a negative energy density, $\pi^2\hbar c/720d^4$ between plates a distance d apart: about 43 kJ/m³ at d = 10 nm, below which real plates stop behaving as perfect conductors. Collecting the energy of Equation 14 at that density would take a stack of 10 nm cavities filling a cube some 300 astronomical units on a side. Macroscopic quantum tunnelling is also real, and was recognised by the 2025 Nobel Prize, but what tunnels is a collective electrical variable of a Josephson circuit through a barrier in its own phase space. For a body of mass m crossing a spatial barrier of height U and width L the amplitude falls as $\exp(-L\sqrt{(2mU)}/\hbar)$, and for an airliner the exponent is a number with more than thirty digits. These effects share words with the commentary. They do not share orders of magnitude [28]. One caveat is carried from §7.7. The comparison treats a 10 nm energy density and a 30 m throat as the same kind of quantity, and there is at least one formulation in which they are not [39]. That does not shrink the gap; it says the gap has not been computed in that formulation.

A second released document, “Quantum Tomography of Negative Energy States in the Vacuum” (11 January 2011), supplies the instrument. It records that sub-vacuum energy density has been made in the laboratory in two forms only, squeezed light and Casimir cavities, and in small amounts; that balanced homodyne detection measures the first, at the 6 to 7 dB below vacuum noise of the experiments it reviews; and that nobody had yet measured the second inside a cavity. It recommends a portable time-domain homodyne detector, and arrays of them, to map negative-energy regions around an aerospace platform that engineered spacetime for propulsion. That is a specification for a measurement nobody has reported. It is not a report of one. Its value here is that the conditioned-vacuum claim of §10 acquires a defined observable — field-quadrature noise below the vacuum level in the near field of the object — and that a camera, thermal or optical, is not the instrument that sees it [30].

What an IEC-class well *can* do, if one stays inside published behavior, is store electrostatic and kinetic energy in a small volume and dump it along an axis when the well is made asymmetric. Three wells walked toward one another — $\mathrm{d}r/\mathrm{d}t < 0$ in Equation 1, with the spin-up of Equation 9 — would raise energy density at the centroid. Reconnection and well-merger on the flight axis would look, on a thermal plate, like a sudden column and then an empty frame. That is a possible reading of the flash. It is not a demonstration that spacetime opened.

If someone still wants the stronger reading — that the merged well is a pocket of conditioned vacuum in Pais’s sense — the only honest placement for that pocket is the same place the geometry already points: the centroid, at the moment of closest approach, along $+x$. Pais’s own version places a fourth source at the destination, which is why Plate I shows three and not four.

That version costs nothing in the clips, and an unobservable fourth body cannot count as support. It does, however, turn the triad into a pointing instrument, and pointing can be measured. Three sources fix a plane; a fourth fixes a line; the natural geometry is that the normal to the triad through its centroid is the line to the fourth source. A destination on the Earth at great-circle distance D lies along a chord that dips $D/2R_E$ below the local horizontal: 4.5° for 1000 km, 45° for a quarter of the way round the globe, straight down for the antipode. A triad spinning in a plane exactly normal to a level flight axis points at the horizon, which is to say at no terrestrial destination. So the destination reading predicts that in the locked phase the plane of the triangle tilts away from the fuselage normal, by an angle and toward an azimuth that together name a place. That is the tilted, precessing plane of Equation 5 with $\delta_i = 2\pi i/3$ brought to rest, and a side view or the ellipticity of the projected triangle would show it. No tilt, no terrestrial address. The suggestion stops there.

The author's own work sits in aneutronic sources. That is why this section exists, and why it is written as a candidate rather than a finding. The next measurement is still stereo. A second measurement, if the files survive stereo, would be any signature that the compact sources have a non-Maxwellian core or a discrete channel structure — the two things an IEC would be expected to show and a painted overlay would not.

12. A second candidate core — the pulsed Z-pinch

The IEC of §11 is one laboratory object that could sit at a vertex. A second has been proposed in discussion of this paper and deserves the same treatment: state it, keep what is physics, cost it, and say what is left. It is a speculative architecture, referred to here as MECPS, for a MIFTI-encapsulated cylindrical propulsion system. It is offered, like §11, as a suggestion only.

12.1 The proposal

The reference case is not the orb but the "Tic-Tac" of the November 2004 USS Nimitz encounter: a smooth white oblong about 12 m long, with no wings, plume or visible means of lift, to which radar operators and aircrew attributed accelerations far outside any known airframe. Knuth, Powell and Reali, working from the reported radar descent of some 8.5 km in 0.78 s, put the implied acceleration in the thousands of g [33]. (Some retellings add "60 miles in one second"; the witness accounts describe reappearance at a point about 60 miles away in well under a minute, which is remarkable enough and should be quoted as given.)

MECPS imagines that object as built hardware. The core is a staged Z-pinch of the kind developed by Magneto-Inertial Fusion Technologies, Inc.: a puff of heavy gas, krypton or xenon, is driven inward by a multi-megampere current pulse and compresses a deuterium or deuterium–tritium target on the axis. The hull is a seamless high-pressure cylinder of the class made for industrial gas storage at up to 1000 bar, 12 m by 1.5 m, holding the driver, the gas reservoirs and superconducting coils. Thrust is a pulsed plasma jet accelerated by the Lorentz force at about 10^5 m/s, at 10 to 100 pulses per second and 10 to 100 MJ per pulse. A rotating plasma ring at each end is proposed as a "warp emulator" producing a small subluminal metric bubble, and various dampers are invoked for inertia, heat and signature.

12.2 What in it is real: the staged Z-pinch

The core is the real part, and it has a longer pedigree than most of what this paper discusses. The staged Z-pinch came out of Norman Rostoker's plasma physics laboratory at the University of California, Irvine, the same laboratory that produced the field-reversed-configuration program now at TAE Technologies (§9.1). Its originator is Hafiz Rahman, and the first paper is Rahman, Wessel and Rostoker in *Physical Review Letters* in 1995; nine further

papers in *Physics of Plasmas* and elsewhere run to 2021 [32]. The company formed to develop it is Magneto-Inertial Fusion Technologies, Inc. (MIFTI Fusion).

The mechanism is specific. In a classic Z-pinch an axial current J_z makes an azimuthal field B_θ that squeezes the column, and the column promptly kinks and sausages apart. In the staged pinch the current runs in a liner of high atomic number — argon, krypton or xenon gas, or solid copper, silver or tantalum — that surrounds a low-Z target of deuterium or deuterium–tritium, with a modest axial field B_z threaded through both. The liner implodes. Shock waves stagnate at the liner–target interface and form a secondary piston that compresses the target; the same shocks preheat it; and the azimuthal field diffuses through the liner to the interface. The liner goes unstable, as liners do, while the target inside it stays intact. The company's time-resolved images of shot 5230, a krypton liner on deuterium with B_z = 1.0 kG, follow the column from 67.7 to 116.4 ns through stagnation, and that stability is the claim on which everything else rests. Figure 5 shows the sequence.

Figure 5. How a staged Z-pinch works: three moments in one shot (longitudinal section, not to scale)

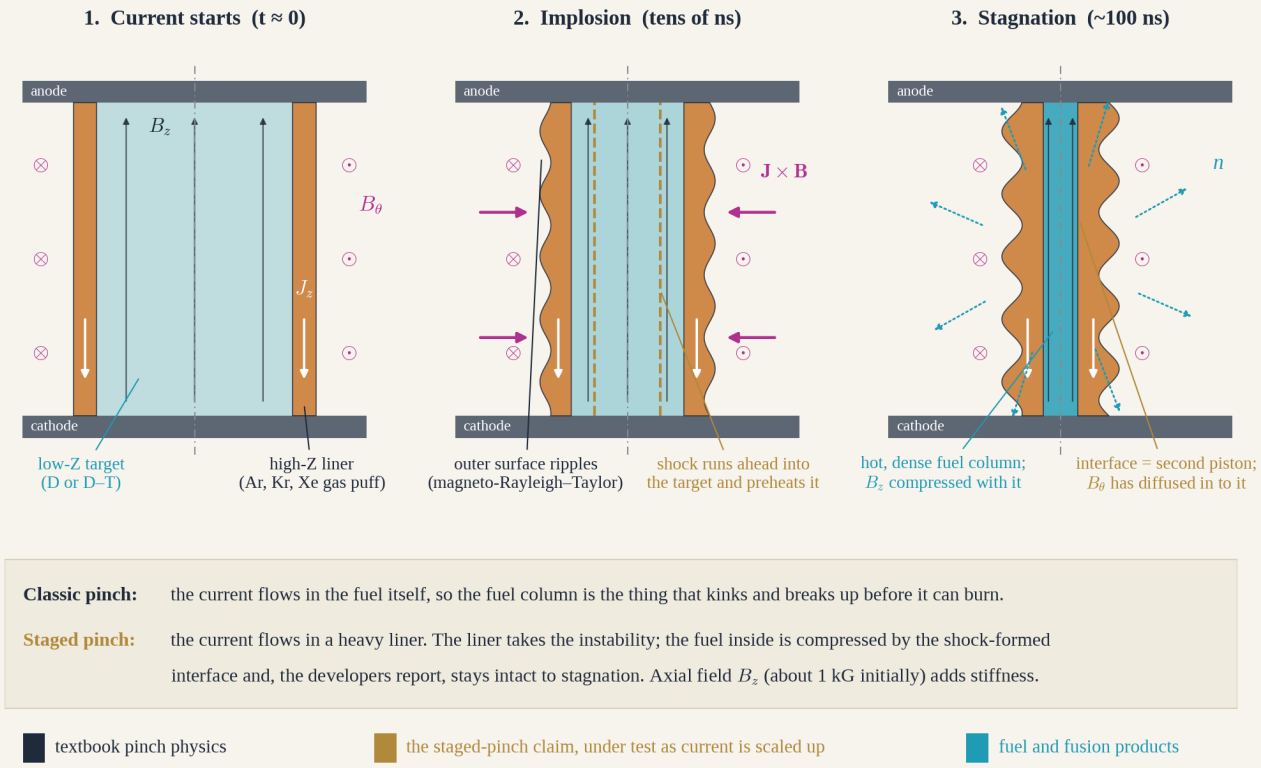


Figure 5. The staged Z-pinch in three moments, drawn for this paper from the developer's published description [32]. Conventional current runs from anode to cathode in the liner; its azimuthal field drives the liner inward; the fuel is compressed inside it. Proportions and timings are indicative. Gold marks the part of the account that is the staged-pinch claim rather than textbook physics.

The experimental record is a ladder of borrowed machines, each compared with magnetohydrodynamic simulation beforehand in HYDRA (Lawrence Livermore), MACH2 (Sandia and Los Alamos) and the open-source FLASH code (Chicago, now Rochester). MACH2 is a two-dimensional code, and the kink that limits a pinch is three-dimensional; for the reason given in §7.7, the three-dimensional runs are the ones that bear on stability:

Facility	Peak current	MHD-predicted D–D neutrons	Measured	Fusion energy per shot	Status
CESZAR, UC San Diego	0.5 MA	10^{8}	10^{8}	~0.1 mJ	Done; upgrade to 1 MA planned
Zebra, University of Nevada, Reno	1.0 MA	10^{10}	10^{10}	~12 mJ	Done
Double-EAGLE, L3Harris	3.5 MA	10^{11}	10^{11}	~0.12 J	Done
Quad Eagle, Fisica	7 MA	10^{13} (thermonuclear)	—	~12 J	New machine; campaigns planned
Modular 12 MA LTD machine	12 MA	10^{15}; breakeven in D–T	—	~1.2 kJ in D–D; a few hundred kJ in D–T	Design; target 2030

Table 4. The staged Z-pinch experimental ladder as stated by MIFTI Fusion (company presentation, September 2025, cited with permission) [32]. Energies are computed here from the neutron counts at 3.65 MeV per D–D reaction with half of reactions yielding a neutron. Rows four and five are targets and projections, not results.

Beyond the 12 MA machine the company's roadmap shows MIFGEN, a compact power plant, in 2035. The 12 MA design is five linear transformer driver modules of five cavities each, feeding a vacuum-insulated centre section through deionised-water transmission lines. The science team is Dr Hafiz Rahman (president and chief scientist; UC Irvine, UC Riverside, TAE), Dr Emil Ruskov (vice president for R&D; Princeton Plasma Physics Laboratory, TAE) and Paul Ney (MHD code development). The science advisory board is Dr Farhat Beg (UC San Diego), Dr Jonathan Feng (UC Irvine), Dr Robert Rosner (University of Chicago), Dr Rick Spielman (formerly University of Rochester, and chief scientist of the Z machine at Sandia) and Dr Sasha Velikovich (formerly of the Plasma Physics Division, U.S. Naval Research Laboratory). Spielman's field is pulsed power and Velikovich's is the gas-puff Z-pinch, which are the two things this concept most needs to get right. On intellectual property, one U.S. patent on the staged Z-pinch was located for this paper, US 9,839,111 B2; the company states that it is extending its portfolio.

One thing must be said plainly. MIFTI's program is fusion energy. Nothing in its materials proposes a propulsion system or says anything about aerial phenomena, and none of the people named above has reviewed, contributed to or endorsed this paper. MECPS is an extrapolation made here, from their published physics, and they bear no responsibility for it. The author has no financial interest in MIFTI Fusion.

The Z-pinch is also the natural fusion geometry for propulsion, because it is already a cylinder with an axis along which plasma can leave, which is why pinch engines recur in the NASA advanced-concepts literature. Pulsed plasma thrusters fly today. Seamless 1000-bar vessels are catalogue items. The distance between this and a flying object is one of scale, and the scale can be computed.

12.3 The arithmetic

Start with the yield, using Table 4. The best measured shot, 10^{11} D–D neutrons at 3.5 MA, is about a tenth of a joule of fusion energy. The 10^{13} of Quad Eagle, which some accounts of this concept describe as validated, is a target for a machine whose campaigns lie ahead, and would be about 12 J. The company's own breakeven projection at 12 MA is of order a few hundred kilojoules in D–T, single shot, in 2030. The MECPS design pulse is 50 MJ at 50 Hz. So the proposal asks for roughly two hundred times the yield of the developer's most ambitious stated milestone, fifty times a second, in a hull 12 m long. It is also inconsistent with itself: a 50 MJ D–T pulse is 1.8×10^{19} neutrons, not 10^{15}; and a cylinder 12 m by 1.5 m encloses 21 m³, not 150.

The ladder deserves one careful remark. Yield rose a hundredfold from 0.5 to 1 MA and tenfold from 1 to 3.5 MA. These are different machines with different rise times and loads, not a controlled scan, so no exponent should be

read off them. But the next step, a hundredfold for a doubling of current, is steep, and it is the measurement that will decide the concept. The company's own phrase for Quad Eagle is that it should definitively prove the scaling. That is the right experiment, and a reader of this paper should watch for its result before weighing anything built on top of it.

Next the driver. A 12 MA pulse needs several megajoules stored and delivered in about 100 ns. At the roughly 1 kJ/kg of fast pulsed capacitors that is several tonnes of capacitor before switches, insulation and transmission line. Linear transformer drivers are the most compact architecture known, and the 12 MA design above is still a star of five modules and water lines many metres across: a ground facility, as its designers intend. Recharging at 50 Hz is hundreds of megawatts through the power electronics. Nothing here is forbidden. Nothing here is yet 12 m long.

Then the motion. For any reaction drive the jet carries away power

$$P_{\text{jet}} = \tfrac{1}{2} F v_e = \tfrac{1}{2} \dot{m}\, a\, v_e, \qquad \frac{m_p}{m} = 1 - e^{-\Delta v / v_e}$$

Equation 15. Jet power of a reaction drive at thrust F and exhaust speed v_e, and the propellant fraction for a velocity change Δv.

Take the proposal's own burst, 0 to 7000 mph in 0.1 s, for a 20-tonne vehicle. That is 3190 g and a thrust of 6×10^8 N. The kinetic energy delivered is 98 GJ, a mean power of about 1 TW, already ten times the 100 GW claimed. But at an exhaust speed of 10^5 m/s the jet power of Equation 15 is 31 TW for that tenth of a second: about 63,000 pulses of 50 MJ, delivered in the time allotted to five. The propellant is not the problem — about 616 kg of the 1000 kg aboard — the power is. High exhaust speed saves mass and spends energy, and this design sits far out on the expensive side of that trade. No arrangement of coils changes Equation 15. It is momentum conservation.

Then the air and the crew of the other aircraft. At Mach 5 at sea level a 1.5 m body dissipates about 1.6 GW in drag and sees a stagnation temperature near 1728 K; it glows in the infrared and drags a shock. A plasma exhaust that "recombines in mid-air" radiates its recombination energy and is bright, not invisible. And 2.5 GW of D–T fusion is 9×10^{20} neutrons per second. Unshielded, that is of order 0.4 Gy per second at one kilometre. The Nimitz pilots closed to well inside that and flew home. Shielding 14 MeV neutrons takes a metre-class thickness of hydrogenous material and tens of tonnes. The aneutronic route of §9.1 and §11 is the only one compatible with the witnesses' health, and it is further from breakeven still.

12.4 What does not survive

Several elements of the proposal are not engineering gaps. They are terms without operational content, and a paper that asks to be falsified should say so. Two can be checked by formula:

$$\omega_{LT} \simeq \frac{2GJ}{c^2 r^3}, \qquad T_U = \frac{\hbar a}{2\pi c k_B} \approx 4 \times 10^{-21}\ \text{K per m/s}^2$$

Equation 16. Lense–Thirring frame-dragging rate at distance r from angular momentum J, and the Unruh temperature at proper acceleration a.

A plasma ring of 1 kg at 1 m radius spinning at 10^6 rad/s drags frames at about 1.5×10^{-21} rad/s: a rotation of one radian in twenty trillion years. It does not emulate a warp bubble. The "-10^{-3} J/m³" of negative energy assigned to it has no derivation and, against the 10^{16} J/m³ and more that even optimistic warp estimates require, would not matter if it did. The Unruh temperature at 1000 g is 4×10^{-17} K. It is not a heat load, and nothing needs cooling from it. "Hawking-like dampers", stabilisation by "AdS/CFT holography", inertial damping by gyroscopes, and negative energy from "fermion baths" do not correspond to any mechanism in the literature those names come from.

Gyroscopes fix orientation; they do not cancel the force on a body that accelerates. The equivalence principle allows one way only to accelerate without feeling it, which is free fall in a gravitational field, and that returns the problem to the mass budget below.

One idea in this group is better than its presentation. A *subluminal* warp shell that needs no negative energy does exist in the literature: Bobrick and Martire in 2021, and Fuchs and colleagues in 2024, constructed warp geometries from ordinary positive-energy matter. The catch is the matter. The published shells are metres across and carry planetary masses, and the solutions move at constant velocity; nobody has shown how to accelerate one except by pushing on it in the ordinary way [34]. That is a real and recent result and it belongs with the hopeful items of §17.1. It is not something a plasma ring can stand in for.

12.5 What is left for the triad

Strip the proposal to what survives and it is this: a compact pulsed fusion core with a preferred axis. As a candidate for a vertex of Equation 1 it has two attractions. If staged-pinch gain is ever reached, the few megawatts per vertex that §7.6 asks for is a modest average power, a few 50 MJ pulses per minute rather than per second. And a pinch has an axis along which plasma leaves, which rhymes with the axial plume of Plate III as the jet mode of the IEC does. Against it: the driver mass, and the fact that the published object is a cylinder of metres, not the metre-class sphere of the plates and of the Gulf of Oman file.

What makes it worth a section is that it is testable on footage in a way the IEC is not. A pulsed core is pulsed. A source firing at 10 to 100 Hz flickers, and against a 24 to 60 frame-per-second camera the flicker aliases into a slow beat in brightness whose frequency follows the repetition rate. Multi-megampere pulses are also among the loudest broadband radio emitters that can be built, so an aircraft nearby would hear each shot across its receivers. A photometric time series of each orb, and any radio log from the night, are therefore tests of this candidate specifically. A steady light curve counts against it.

12.6 A related concept in circulation

A graphic circulating on social media in 2026 under the title “KSM Rocket Booster / Engine — FRC-EVO Maximum Efficiency” belongs to the same family, and sorting its labels is a useful exercise in the method of this section; Figure 6 redraws it as a schematic with the labels sorted. The original shows a cutaway cylinder with plasma rings on the axis and a bright exhaust. Several labels name real things. Field-reversed-configuration plasmoids are the subject of §9. The dense plasma focus is a genuine pinch device, and one private group pursues proton–boron-11 with it. A rotating liquid-metal liner is an old and respectable idea, from the Naval Research Laboratory’s LINUS experiments of the 1970s to General Fusion today. A magnetic nozzle is the standard way to turn charged fusion products into thrust, and “clean helium exhaust” is simply correct for p–^{11}B, whose products are three alpha particles. “Zero neutrons” is not: side reactions such as $^{11}\mathrm{B}(\alpha,n)^{14}\mathrm{N}$ put something like a thousandth of the energy into neutrons, which is small and is not zero.

Figure 6. Schematic longitudinal section of the “KSM” engine concept, labels sorted by status

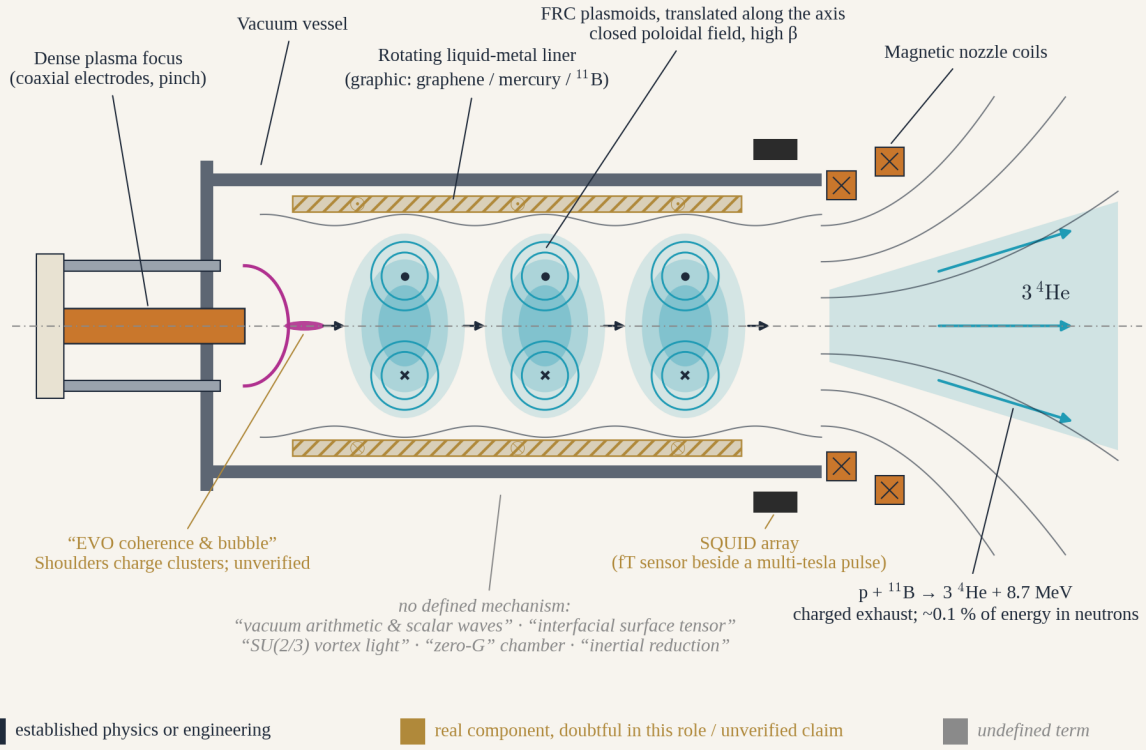


Figure 6. Schematic longitudinal section of the “KSM” engine concept, redrawn for this paper from the labels of the circulating graphic, with the layout rationalised so that source, plasmoid chain and nozzle lie in order along the axis. It is a diagram of a proposal, not of hardware; no dimensions, currents or yields were given and none are implied. Labels are coloured by status.

The remaining labels do not name anything that can be costed. “EVO coherence and bubble” refers to the exotic vacuum objects proposed by Kenneth Shoulders, charge clusters reported in spark discharges whose claimed properties have not been independently established. “Vacuum arithmetic and scalar waves”, an “interfacial surface tensor”, “SU(2/3) vortex light”, a “zero-G toroidal vacuum chamber” and “inertial reduction” have no definitions from which a number could be derived, and SQUID magnetometers, which resolve femtotesla fields, cannot serve as feedback sensors beside a multi-tesla pulsed plasma. The graphic is unattributed and carries no dimensions, currents or yields, so there is nothing in it to test. It is mentioned because it shows the pattern this paper is trying to work against: a real core, a real fuel, a real nozzle, and then a layer of vocabulary where the mechanism should be. The remedy is the same as in §12.4. Keep the pinch, the plasmoid and the nozzle; ask each remaining word for an equation; and let go of the ones that have none [36].

13. A third candidate — the buoyant plasmoid

A third proposal reached the author as a long tutorial titled “Plasma Buoyancy and Trans-Domain Flight: A Classroom Discussion” (April 2026), of unstated authorship [37]. Its central idea is different in kind from the two cores above, and part of it is both correct and directly relevant to a paper about luminous spheres in open air. It deserves to be separated carefully from the rest.

13.1 The idea, and what is right in it

The proposal is lift without thrust. Wrap a hull in a shell of hot, ionised, low-density gas; the denser atmosphere outside then pushes the whole assembly upward, as water pushes a bubble. The tutorial is careful about the first-order physics, and it is worth repeating because it is often got wrong. The shell is not a vacuum. It is at roughly ambient pressure, because a hot gas has fewer particles per volume, each moving faster, and pressure is the product. Low density and full pressure are what a hot-air balloon has, and the shell is a hot-air balloon without the envelope. The tutorial is equally clear that the state is not free: the atmosphere works continuously to cool and mix the shell, so it must be fed continuously. That is the conclusion of §7.6 reached from the other side.

What makes this more than an analogy is that the laboratory object exists. Ohtsuki and Ofuruton in 1991 produced free-floating plasma fireballs in air at atmospheric pressure by microwave interference, and Dikhtyar and Jerby in 2006 ejected buoyant, luminous, roughly spherical fireballs from a microwave-heated hot spot and watched them rise and drift [37]. These are centimetre objects fed with kilowatts, and they last as long as the feed does. But of everything in §9 they are the nearest published thing to a self-luminous orb in the open atmosphere. An FRC needs a vacuum vessel. An IEC is a vacuum vessel. A microwave-sustained plasmoid needs only air and power, and it is bright in the infrared, as the sources in Plate I are. They are also a hundred times smaller, and §7.7 gives the reason the step from centimetres to metres is not free.

13.2 What Archimedes allows

Buoyancy is the one force in this paper with a hard, simple ceiling:

$$F_b = (\rho_a - \rho_p)\,Vg \;\le\; \rho_a V g, \qquad a_{\max} = \frac{\rho_a V g}{\tfrac{1}{2}\rho_a V} = 2g, \qquad \vec{F}_b \parallel -\vec{g}$$

Equation 17. Buoyant force on a volume V of density ρp in air of density ρa; the greatest acceleration buoyancy can give a sphere, allowing for the added mass of the air it must push aside; and its direction.

Three consequences follow, and none depends on how the plasma is made. First, the lift cannot exceed the weight of the air displaced, however hot the shell. A sphere of 1 m radius displaces 5 kg of air at sea level and 1.6 kg at cruise altitude; a shell reaching out to 2 m displaces 41 kg and 13 kg. That is the whole payload, hull included. Second, even a weightless bubble accelerates at no more than 2 g, because it must set the surrounding air moving, and it then rises at a terminal speed of order 7 m/s for a metre-scale sphere. The circle of Equation 1 asks for 10 g and the Nimitz reports for thousands. Third, and decisively for steering, the buoyant force on any closed surface in a fluid at rest points straight up, whatever the shape of the surface. Making the shell thicker on one side moves the centre of buoyancy and tilts the craft. It cannot push it sideways. “Asymmetric buoyancy” is not available as a means of horizontal flight; the tutorial’s own analogy of the lopsided beach ball rises crooked because of drag and torque, not because buoyancy has acquired a sideways component. Under water the numbers grow eight-hundredfold, 4 tonnes of lift for the 1 m sphere, and the same three statements hold.

For the triad this gives a clean discriminator. A buoyant plasmoid drifts with the local air and rises slowly. It cannot hold station on an aircraft moving at 250 m/s, let alone orbit it. So buoyancy may explain why a luminous sphere *floats*, in reports where one does, and cannot explain anything that Plates I and II are claimed to show. If the orbs of the clips are real they are not flying by this means.

13.3 The supporting mechanisms, costed

The tutorial builds its shell from a list of effects, each of which is real, and the difficulty in each case is magnitude or relevance rather than existence. A Townsend avalanche is how a high-voltage surface breaks air down, and it gives corona and streamers. Oxygen does absorb strongly at 60 GHz, about 15 dB per kilometre at sea level, which is an e-folding length near 300 m: the energy is deposited over a city block, not in a sheath at the skin. The 1.42 GHz line is the hyperfine transition of atomic hydrogen, a magnetic-dipole transition with a lifetime of ten million years in a gas of which air contains essentially none; it cannot organise an air plasma. The Debye length in an atmospheric-pressure discharge, at 10^{18} electrons per m³ and 1 eV, is about 7 μm; it sets the scale on which charge is screened, not the thickness of a shell. Solitons are genuine solutions in plasmas, but Russell's canal wave ran a mile because the canal barely dissipated it, and air plasma recombines in microseconds (§7.6). Hastelloy is a fine alloy and is not the hard part.

Power is. To keep a shell hot while moving, the craft must heat the fresh air it sweeps up, at a rate $\rho A v \Delta h$. For a 2 m shell radius, 3 MJ/kg to reach a tenth of ambient density, and cruise conditions, that is about 4 GW, against the 15 MW the tutorial budgets. The proposed source does not close the gap. Thermionic conversion is real and flew on the Soviet TOPAZ reactors, which were fission reactors of about 5 kW electrical and a tonne each, at efficiencies of 5 to 10 per cent; 15 MW at that specific mass is thousands of tonnes. A decay-heat source is further off: plutonium-238 gives 0.57 W per gram, so 15 MW electrical at ten per cent needs some 260 tonnes of an isotope whose world stock is measured in kilograms, and thorium-232, with a half-life of fourteen billion years, gives about three billionths of a watt per gram. For the phase above the atmosphere the tutorial turns to Pais, whose stated flux of 10^{33} W/m² is the output of two and a half million Suns through each square metre; §10.4 has said what needs saying, and the Haisch–Rueda–Puthoff inertia hypothesis it also invokes is a published conjecture without experimental support.

13.4 What the idea becomes when costed

Two real technologies are what remains when this proposal is held to numbers, and both are worth a reader's time. Depositing energy in the air ahead of a fast body does reduce its drag: a heated, rarefied channel weakens the bow shock, and the effect has been measured in wind tunnels with lasers, microwaves and discharges for thirty years. It saves a fraction of the drag at a cost in deposited power; it does not abolish the momentum exchange of §7.5. And a body can travel through water inside a gas cavity: supercavitating torpedoes do it in service, at several times the speed of any conventional one. The cavity is made by speed and injected gas rather than by plasma, entry still makes a splash, and the water still has to be pushed out of the way. Those are the honest descendants of "the craft makes the medium move it", and they are interesting enough [37].

14. Steering — fields, software and intention

Sections 11 to 13 asked what could sit at a vertex. This one asks what could move it. Three answers have been put to the author: radio-frequency fields, as in a recent dual-frequency thruster concept; artificial intelligence; and consciousness, as in the author's own earlier unpublished protocol for a consciousness-coupled plasma vehicle [38]. Each has a version that is real and a version that is not, and the real versions turn out to connect.

14.1 What radio-frequency fields can and cannot push

Radio waves carry momentum, and the amount is fixed:

$$F_{\mathrm{rad}} = \frac{P}{c} \approx 3.3 \text{ N per GW}, \qquad I_{\mathrm{bd}} = \frac{E_{\mathrm{bd}}^2}{2Z_0}, \qquad N_{\mathrm{bits}} \simeq \left(\frac{3}{2\varepsilon}\right)^2$$

Equation 18. Radiation force of a beam of power P; intensity at which a field of amplitude E_bd breaks down air, with Z0 = 377 Ω; and the number of binary trials needed to read one command bit at three standard deviations from a channel whose hit rate exceeds chance by ε.

Three newtons per gigawatt is not a steering force for anything in this paper. What RF does well is make and heat plasma, and the plasma then pushes on something else. In vacuum that is a thruster. The concept paper the author was sent, a student proposal from Virginia Tech, is a good example of the honest form of this idea: a CubeSat engine burning sublimed naphthalene, a measured baseline of 1.1 mN at 45 W and 37 s of specific impulse from Lee and co-workers, a specific hypothesis that a second frequency coupled to helicon and soliton modes will recover dissociation energy now lost as heat, a target of 55 to 150 s, and a stated experiment that could come out negative. The vocabulary is the same as the tutorial of §13 — two frequencies, solitons, Debye length — and the difference is that here each word is attached to a measurement. Such thrusters can be steered: bending the field of the magnetic nozzle deflects the exhaust, and this has been shown in the laboratory. But the scale is millinewtons, in vacuum, with propellant aboard. In air, the real technology is the plasma actuator and its cousin the ion-wind engine: MIT flew a 2.5 kg aeroplane with no moving parts in 2018 on about 3 N from 600 W. Silent, solid-state, steerable, and good for about a tenth of a g against the ten to forty that §7.1 requires [38].

14.2 The orb as a place, not a thing

There is one way in which RF steering changes the argument of this paper, and it comes from §13. The fireballs of Ohtsuki and Ofuruton formed where interfering microwave beams made the field strongest, and they moved when that maximum moved. A plasma sustained by beams is not a body that must be pushed. It is a location that is being lit. Move the focus with a phased array and the luminous spot follows at once, with no inertia, because nothing massive goes anywhere; the air at the new place lights and the air at the old place goes dark in the microseconds of §7.6. Such a spot can turn a right angle, stop dead, or cross the sky faster than any aircraft, as the dot of a laser pointer can. The idea is in the patent record: the U.S. Navy holds US 11,359,892 B2 (2022) on laser-induced plasma filaments drawn in mid-air as infrared decoys for aircraft, and femtosecond-laser plasma has been used to draw touchable images in air [38].

For the triad this is the first candidate in the paper that dissolves §7 rather than failing it. Three spots on a circle about a fuselage is a simple pattern for an array. No centripetal force is needed, no binding, no Routh instability, no wake, no sonic boom and no drag power, because no momentum is carried. The cost moves elsewhere. Breaking down air at cruise altitude takes about 7×10^5 V/m, which by Equation 18 is some 7×10^8 W/m² at the focus; sustaining a plasma takes less, but a metre-sized microwave focus at 10 km needs an aperture tens of metres across even at 94 GHz. Ultrashort laser pulses reach breakdown with watts of average power, which is why the Navy patent uses them, and their spots are small and faint by comparison with Plate I. The candidate also makes sharp predictions that a body does not. The spots brighten and flicker at the pulse rate of the source. They go out wherever the airframe shadows a beam, so a spot circling a fuselage must show a dead sector fixed relative to the emitter, not to the aircraft. They are hot in the infrared, never cold. And through any tightening of the pattern, ωr^2 has no reason to be conserved. That last point needs saying plainly, because it revises §7.3: constant ω through the collapse is what an animation would show, and it is also what a projected pattern would show. Equation 9 separates bodies from non-bodies. It does not by itself separate a projection from a forgery; the shadowed sector and the pulse flicker do. None of this makes an airliner disappear, and a projected plasma has no bearing on §11.4.

14.3 Software at the controls

Artificial intelligence as a means of steering needs no speculation at all, and §7.2 shows why it would be required. A formation that is unstable in every passive version is a control problem. Whether the vertices are craft holding station or foci being placed, something must close the loop faster than the instability grows, in three dimensions, on noisy sensing. The state of the art is directly relevant: in 2022 a deep reinforcement-learning controller, trained in simulation, took over the nineteen magnetic coils of the TCV tokamak in Lausanne and held, shaped and even split a fusion plasma at ten thousand control cycles per second. Steering a plasma by learned policy is a published result. The same methods fly drone swarms in formation. If the triad of Equation 1 is ever built, by anyone, of anything, this is how it will be held.

14.4 Intention

Consciousness can steer a vehicle today, in one well-defined sense. A brain–computer interface reads the electrical correlates of intention and turns them into commands. People with implanted arrays have moved robotic arms and written text at ninety characters a minute; with nothing more than a cap of scalp electrodes, volunteers have flown a quadcopter through an obstacle course by imagining hand movements. The channel is narrow, around a bit per second from the scalp and some tens from an implant, so the practical architecture is a hierarchy: the person supplies intent, where to go and what to look at, and software of the kind in §14.3 supplies the thousands of corrections per second. Intention, interface, controller, phased array, plasma: every link in that chain exists. That is a real and rather beautiful answer to the question, and it asks nothing new of physics.

The stronger sense is different, and the author's earlier protocol relies on it: that coherent intention acts on matter directly, biasing random-number generators by many standard deviations, ionising air through the body's own fields, and, through the orchestrated objective reduction of Penrose and Hameroff, coupling to spacetime. The record has to be given as it stands. The Princeton laboratory that reported intention effects on random generators measured a shift of about one part in ten thousand per bit; the three-laboratory replication it took part in did not reproduce the effect, and the largest meta-analysis found an effect that small studies carry and large ones do not, the usual mark of selective publication. Suppose the effect real at its claimed size. Equation 18 gives 2×10^{8} trials to read one command bit, sixty hours at the rate those machines ran. No vehicle can be steered at one bit per sixty hours. The fields of the body are microvolts at the scalp and millivolts at the chest, seven orders of magnitude below the three million volts per metre at which air breaks down. And objective reduction, in Penrose's own formula, associates a conscious moment of 25 ms with a gravitational self-energy $\hbar/\tau$ of 4×10^{-33} J. Microtubule quantum effects are a live experimental question, and recent anaesthesia work has kept it open. But the theory's own number stands seventy-eight orders of magnitude from Equation 14. Whatever consciousness is, the route by which it demonstrably reaches a machine today runs through electrodes, and that route is open now [38].

15. Separating the mouths — distance and time

The same discussion extends MECPS from a vehicle into a tug: one mouth of a wormhole pair is carried in the hull to a distant star at 0.99*c*, and a further variant uses the journey to set the two mouths at different times. Pais's fourth source at the destination (§11.4) is the same picture seen from the far end. This section separates the part that is textbook relativity from the part that is not.

The textbook part is striking, and it is not speculation once a wormhole is granted. In 1988 Morris, Thorne and Yurtsever showed that if one mouth of a traversable wormhole is taken on a relativistic round trip, the twin-paradox difference between the two mouths' clocks is preserved through the throat. No second device is needed. A

wormhole whose mouths have been moved apart is already displaced in time, and the offset is set by the trip [35]:

$$E = (\gamma - 1)mc^2, \qquad \frac{m_0}{m_1} = \left(\frac{1+\beta}{1-\beta}\right)^{c/2v_e}, \qquad \Delta t = (\gamma - 1)\,\tau$$

Equation 19. Energy to bring mass m to Lorentz factor γ; rocket mass ratio to reach β = v/c at exhaust speed v_e; clock offset for proper time τ at γ.

The costs follow from the same line. At 0.99*c*, γ = 7.09: a 100 light-year crossing takes 101 years at home and 14 aboard, as the proposal says. Bringing a 50-tonne assembly to that speed takes 2.7 × 10^{22} J, some {M['world_yrs']:.0f} years of present world energy use, or {M['yrs_at_10GW']/1e3:.0f},000 years of the proposal's 500 MJ pulses at 20 Hz. If it is a rocket, the best exhaust speed D–T fusion can give is about 0.087*c*, and Equation 19 then asks for a mass ratio near 10^{13} to accelerate, and its square to stop. Relativistic transport of a mouth is a beamed-energy or field-propulsion problem, not a fusion-rocket problem, whatever the core.

The temporal variant quotes +50 years in seven minutes of ship time on a 10 km orbit at 0.999*c*. At 0.999*c*, γ is 22, and seven minutes aboard is 2.6 hours at home. Fifty years in seven minutes needs γ near 4 × 10^6, which for 50 tonnes is 1.7 × 10^{28} J — the Sun's whole output for about forty seconds — held on a circle whose proper acceleration is 10^{25} g. The "1 to 10 GJ per jump" of the proposal is short by eighteen orders of magnitude. Even at the modest 0.999*c* the orbit pulls 5 × 10^{14} g, and the Unruh temperature there is twenty microkelvin, not the 10^{15} K quoted. A "plasma ergosphere" is excluded by Equation 16.

On causality the literature is richer than the proposal. Once the mouths are offset in time and brought near, closed timelike curves exist, and two real results apply. Novikov's self-consistency principle is a statement about which solutions exist, and the billiard-ball studies of Echeverria, Klinkhammer and Thorne found self-consistent solutions for every initial condition they tried; it is a property of the physics, not a function that qubits enforce. Hawking's chronology protection conjecture, and Kim and Thorne's reply to it, concern whether vacuum fluctuations pile up on the chronology horizon and destroy the machine before it can be used. That question is open, and it is the honest place to leave it [35].

So the sober reading of the bridge is this. Its propulsion, its dampers and its timetable do not survive arithmetic. Its central idea does: given one traversable wormhole, relativity alone turns it into a link across time as well as space, by nothing more exotic than moving one end. Of everything in this paper that is conditional on a wormhole, that is the most remarkable consequence, and it was derived by the people who wrote the textbook.

16. A programme to close the gaps

Parts I and II leave a list of open issues. They are not equally hard, and it is worth sorting them by what it would take to close each one, because several are within reach of a small group and a modest budget.

16.1 Days: the footage

Everything in this paper hangs on a conditional, so the first work is on the clips themselves. With the best available copies each source can be tracked frame by frame to give the rotation period, the angular spacing, the product ωr^2 through any tightening, the tilt of the triad plane from the fuselage normal (§7.7, §11.4), a brightness time series for pulse flicker, and a search for a sector in which a source is shadowed. Those are the tests of §8, and they turn that section from proposals into results. In parallel the cloud-photograph match of §1.1 should be repeated independently, from the stock images, with the registration published. The tracking code and data should be released with the results so that anyone can rerun them.

16.2 Months: two bench experiments

The projected-plasma candidate of §14.2 is the most testable idea in Part II. A microwave-sustained fireball in a chamber held at cruise-altitude pressure, about 0.24 atm, would give the power needed per luminous spot, its in-band infrared brightness for comparison with Plate I through Equation 12, and the speed with which the spot follows a moving focus. A kilowatt-class source and a university plasma laboratory are enough.

The same apparatus supports a second experiment that, so far as the author can find, has not been done: a plasma steered by intention through a brain–computer interface. A scalp-electrode cap supplies the intent, a software controller of the kind in §14.3 supplies the fast corrections, and the focus of the microwave field moves the plasmoid. Every component exists. The result would be the honest form of the bridge between consciousness and physics that §14.4 describes, and it would be a first.

16.3 A question for the pinch

For the staged Z-pinch the deciding data will come from the 7 MA campaign. Three things matter more than the headline yield: yield against current on a single machine, so that a scaling exponent can be read without changing drivers; the split between thermonuclear and beam-target neutrons, from anisotropy and time-of-flight spectra; and shot-to-shot reproducibility. With those three the ladder of Table 4 becomes a curve, and the projection to 12 MA can be judged.

16.4 One experiment worth funding

On the wormhole side there is a first step that is small, real and unclaimed. The reference document on quantum tomography [30] describes measuring sub-vacuum fluctuations inside a Casimir cavity with a balanced homodyne detector, following Marecki’s proposal, and states that the measurement had not been made. It would be the first direct map of negative energy density in the laboratory. It is a tabletop quantum-optics experiment, not a propulsion program, and it is publishable whatever it finds.

16.5 What stays open

Four gaps are not closable now and should be carried as open rather than argued away: the planetary scale of negative energy in Equation 14, unless the small-total constructions of Visser and co-workers can be given a physical source; accelerations of thousands of g without reaction mass; the relativistic transport of a wormhole mouth in §15; and, on the author’s own side, a three-dimensional treatment of the triad’s stability, which Bocker’s tilted inertia tensor (Equation 9b) begins, and a scale-aware recomputation of §11.4 (§7.7). Progress on the first three will come from theory first. The fourth is theory this paper can do next. The items above do not depend on them.

17. Closing

The circulating sequences, taken at face value, describe three objects on a circle about the fuselage, locked 120° apart, optionally breathing along the flight axis on a thin torus. That is a small, testable geometry. It can be drawn, differentiated, and compared with plate scale. It does not require exotic matter to write down, and it does not become exotic matter by being written down. A spherical IEC at each vertex is one way that geometry could be built. It is not the only way, and the clips do not yet choose.

The dynamics are less forgiving than the geometry. The circle demands an inward force of many g, a passive binding of three equal bodies is unstable, a magnetic binding needs fields beyond the laboratory, and the power to

glow and to fly is megawatts per vertex. None of that proves the footage false. All of it is what the footage would have to be true of, and one line of it — ωr^2 constant through the collapse — can be checked on the circulating files this week.

If later work authenticates the files and recovers a coherent depth map, the equations in §4–§7 are the prior one should update, not replace — unless the disparity map shows the objects were never in a plane normal to the jet. If the files fail stereo, or fail Equation 9, the geometry remains a clean description of what the pictures *look like*, which is still the right starting point for anyone who intends to argue about them.

17.1 What remains open

None of this closes the larger question, and it would misread the paper to take it that way. The scepticism above is aimed at a video. It is not aimed at the idea. General relativity has permitted wormhole geometries since Einstein and Rosen wrote one down in 1935, and nothing discovered since has withdrawn the permission. What the theory asks for in return is negative energy, and within living memory negative energy has gone from a mathematical embarrassment to a laboratory quantity: measured between Casimir plates, generated on demand as squeezed light, and used routinely to push the LIGO detectors below the noise of the vacuum itself.

The theory has moved as well. In 2017 Gao, Jafferis and Wall showed that a wormhole can be made traversable by an ordinary quantum coupling between its two mouths, with no exotic matter put in by hand. In 2018 Maldacena, Milekhin and Popov built a traversable wormhole in four dimensions out of ingredients close to the Standard Model. In 2022 the corresponding teleportation protocol was run on a quantum processor. In 2021 and 2024 warp geometries were constructed from ordinary positive-energy matter, with no exotic ingredient at all [34]. And the oldest result of the set is still the most surprising: move one mouth of a wormhole and relativity makes it a link across time as well as space (§15). These solutions are small and slow, or massive beyond any engineering. The known ones take longer to cross than the space outside them, and none is a road an airliner could take. They matter because they change the standing of the question. A traversable wormhole is no longer something physics forbids and fiction supplies. It is something physics permits and engineering cannot yet reach, and that is a familiar place for a technology to stand [31].

The distance is real and belongs in the same breath: the energy of twenty Jupiters, with a minus sign, against laboratory amounts that would not warm a grain of dust. But the total can in principle be made arbitrarily small, the inequalities that would forbid it are unproven exactly where it matters, and the government’s own reference documents conclude not that the thing is impossible but that it needs sustained work and an instrument — and then they specify the instrument [30]. Gaps of this size have closed before. Forty years separated the Curies’ first radioactive salts from Fermi’s pile. A century separated Einstein’s prediction of gravitational waves from the morning they were heard. In each case the gap closed because someone wrote down exactly what would have to be true, and then went and measured.

That is the spirit in which this paper is offered. If the footage is an animation, the tests here will show it, and nothing is lost but an afternoon. If it is not, these equations are the first page of the manual. Either way the work is the same: a disparity pipeline on the original frames, a stopwatch on the collapse, and one day a homodyne detector pointed at a region of space where the vacuum has been persuaded to give way. The geometry of a doorway is simple. Three points fix a plane, and a fourth says where it leads. We do not yet know how to build one. We know, now, what to look for — and the universe has not said no.

Notes and sources

[1] Public circulating corpus associated with MH370 “Gorgon Stare” / thermal sequences, as compiled and commented by Ashton Forbes (@AshtonForbes) and the 4ORBS evidence library, 2024–2026. Stills in Plates I–II were extracted from clips posted to X, including status/2101012125426839712 (thermal, 18 Sep 2026), status/2101098948119437350 (thermal triad, 19 Sep 2026), status/2083409891105165572 (inverted FLIR), and status/2049183874564121014 (overhead optical family). Reproduced here for commentary and geometric reference. Plate III stills: source file posted by @airsuperiorx, status/2053968963034304788 (11 May 2026, “UAP over Ukraine in May of 2025”).

[2] Tuszewski, M. “Field reversed configurations.” *Nuclear Fusion* 28, 2033 (1988). Canonical review of compact, self-organized plasmoid equilibria.

[3] Bussard, R. W. “The advent of clean nuclear fusion: superperformance space power and propulsion.” 57th International Astronautical Congress (2006). Polyhedral cusp / Polywell architecture.

[4] Pais, S. C. US 10,144,532 B2, “Craft using an inertial mass reduction device” (granted 4 Dec 2018; expired for non-payment). US 10,135,366 B2, electromagnetic field generator. US 10,322,827 B2, high-frequency gravitational wave generator. US 2019/0058105 A1, piezoelectricity-induced room-temperature superconductor (abandoned). US 2019/0295733 A1, plasma compression fusion device (abandoned). All assigned to the U.S. Secretary of the Navy.

[5] Pais, S. C. “The Plasma Compression Fusion Device—Enabling Nuclear Fusion Ignition.” *IEEE Transactions on Plasma Science* 47, no. 11 (2019): 5119–5124. doi:10.1109/TPS.2019.2942997.

[6] Pais Effect definition as “controlled motion of electrically charged matter (from solid to plasma) via accelerated spin and/or accelerated vibration under rapid acceleration transients”: Pais writings and subsequent interviews; restated in contemporary reporting (The Drive / The War Zone; Big Think, 2021).

[7] NAWCAD public statement: testing of the Pais Effect / HEEMFG from October 2016 to September 2019, approximately $508,000; “the Pais Effect could not be proven.” Reported by The War Zone and SpyTalk / The Daily Beast, 2021.

[8] Interviews in which Pais discusses the circulating orb sequences: Ashton Forbes / Dave Rossi, “UFO Disclosure w/ Salvatore Pais” (1 Dec 2024); Forbes, “Salvatore Pais Tells All! MH370 Videos, AI, and ZPE” (25 Jan 2025); Forbes, “Hard Truths /w Sal Pais — Felony Physics Edition” (22 Feb 2026); Jesse Michels conversation as circulated in secondary commentary (singularity remarks; fourth source placed at the destination).

[9] On stereo as a falsifier: a genuine two-view record must admit one fundamental matrix and a layered disparity map. See Hartley & Zisserman, *Multiple View Geometry in Computer Vision*, Cambridge.

[10] Aircraft dimensions: Boeing 777-200ER airport planning data (fuselage length, wingspan, tail height).

[11] Beskrestnov, S. (“Flash”). Public release of Unmanned Systems Forces drone video of a six-cone spherical object with heat plume, combat operations, ~800 m. Reported in Kyiv Post, “Senior Ukraine Official Reports Armed Forces Sighted UFO, Publishes Video,” 12 May 2026.

[12] “Ukrainian Military Observations and Analysis of Aerospace Objects and Phenomena during Defense against the Russian Federation.” Open military/academic compilation (Mavic 3T thermal, 8–14 µm): wedge and in-line formations of four–five spherical objects, 2023–2024; objects bright in IR and dark in co-bore optical on 24 December 2024. See also Main Astronomical Observatory of NAS of Ukraine notes on the 406th Battalion Mavic 3T sequence.

[13] Miley, G. H., Nadler, J., Hochberg, T., Gu, Y., Barnouin, O., Lovberg, J. “Inertial-Electrostatic Confinement: An Approach to Burning Advanced Fuels.” *Fusion Technology* 19, no. 3 (1991): 840–845.

[14] Miley, G. H., Gu, Y., DeMora, J. M., Stubbers, R. A., Hochberg, T. A., Nadler, J. H., Anderl, R. A. “Discharge Characteristics of the Spherical Inertial Electrostatic Confinement (IEC) Device.” *IEEE Transactions on Plasma Science* 25, no. 4 (1997): 733–739. Star-mode microchannels through grid openings.

[15] Miley, G. H., Bromley, B. P., et al. US 6,121,569, “Plasma jet source using an inertial electrostatic confinement discharge plasma” (granted 19 September 2000). Jet-mode extraction from a ported spherical IEC; direct-conversion grids for charged fusion products.

[16] Miley, G. H., and Murali, S. K. *Inertial Electrostatic Confinement (IEC) Fusion: Fundamentals and Applications*. Springer, 2014. Compact IEC as an aneutronic (p–^{11}B) candidate; nested wells. (An earlier note in this draft cited Sved as co-author; the 2014 Springer monograph is Miley and Murali.)

[17] Biographical particulars: University of Illinois NPRE faculty profile; ANS Seaborg Medal citation (advanced-fuel / direct-conversion line); Edward Teller Medal, 1995. Figure 4 left is a laboratory IEC vessel of the Urbana class. Figure 4 right is an artist’s conception of a ported IEC-class sphere in flight configuration (illustration signed Vaughan; hull marked Inertial Dynamics), reproduced here as a topology reference, not as a program document.

[18] Counter-evidence on the clips: “The MH370 Teleport Hoax,” *Skeptical Inquirer*, February 2024; community compilation of the August 2023 Pyromania “Shockwave” element comparison and the December 2023 textures.com cloud-photograph match (photographs by Jonas De Ro, 2012), with Forbes’s published rebuttals. Readers should consult both sides’ primary posts; this paper takes the matches as

open challenges the footage must answer, not as settled by citation.

[19] Conventional record: Ashton, C., Shuster Bruce, A., Colledge, G., Dickinson, M. “The Search for MH370.” *Journal of Navigation* 68 (2015): 1–22 (Inmarsat burst-timing and burst-frequency analysis). Australian Transport Safety Bureau, *The Operational Search for MH370* (2017). Flaperon recovered on Réunion 29 July 2015 and attributed to 9M-MRO by French judicial authorities, September 2015.

[20] Routh, E. J. “On Laplace’s three particles, with a supplement on the stability of steady motion.” *Proc. London Math. Soc.* 6 (1875): 86–97. Modern treatment in Danby, *Fundamentals of Celestial Mechanics*. Stability of circular orbits under power-law forces: Goldstein, *Classical Mechanics*, ch. 3.

[21] Normal modes of the equilateral X_3 system: Herzberg, G. *Infrared and Raman Spectra of Polyatomic Molecules* (1945). The mode frequencies and the √2 ratio in Equation 8 were also checked numerically for this paper.

[22] Dipole–dipole force and dipole fields: Jackson, J. D. *Classical Electrodynamics*, 3rd ed., ch. 5. Continuous-field record of about 45 T: National High Magnetic Field Laboratory hybrid magnet.

[23] Morris, M. S., and Thorne, K. S. “Wormholes in spacetime and their use for interstellar travel.” *Am. J. Phys.* 56 (1988): 395–412. Visser, M. *Lorentzian Wormholes* (AIP, 1995). Ford, L. H., and Roman, T. A. “Averaged energy conditions and quantum inequalities.” *Phys. Rev. D* 51 (1995): 4277.

[24] Schwinger, J. “On gauge invariance and vacuum polarization.” *Phys. Rev.* 82 (1951): 664. Vacuum magnetic birefringence searches: PVLAS collaboration.

[25] Atmosphere at 35,000 ft (ISA): density 0.380 kg/m³, pressure 23.8 kPa, speed of sound 296.5 m/s. All numerical values in §7, §10.4 and §11.4 were computed from the stated formulas with m = 100 kg and R = 1 m as placeholders, not measurements.

[26] Lockheed Martin Compact Fusion Reactor: Chase, C., Solve for X presentation, 7 February 2013. Norris, G. “Skunk Works Reveals Compact Fusion Reactor Details.” *Aviation Week & Space Technology*, 15 October 2014. McGuire, T. J. US 9,934,876 B2 and US 9,947,420 B2, “Magnetic field plasma confinement for compact fusion power”; McGuire, US–Japan Compact Torus Workshop presentation (2016), T4/T4B parameters. T5 statement by J. Babione reported by The War Zone, July 2019. Trimble, S. “Skunk Works Halted Nuclear Fusion Effort Before 2021.” *Aviation Week*, 30 August 2023.

[27] TAE Technologies FRC program: Binderbauer, M. W., et al. “A high performance field-reversed configuration.” *Phys. Plasmas* 22, 056110 (2015). Limits on thermal p–^{11}B: Rider, T. H. “Fundamental limitations on plasma fusion systems not in thermodynamic equilibrium.” *Phys. Plasmas* 4, 1039 (1997).

[28] Casimir, H. B. G. *Proc. K. Ned. Akad. Wet.* 51, 793 (1948). Wilson, C. M., et al. “Observation of the dynamical Casimir effect in a superconducting circuit.” *Nature* 479, 376 (2011). Nobel Prize in Physics 2025 (Clarke, Devoret, Martinis): macroscopic quantum tunnelling and energy quantisation in an electric circuit.

[29] U.S. Department of War, PURSUE (Presidential Unsealing and Reporting System for UAP Encounters), war.gov/UFO: six releases, 8 May, 22 May, 12 June, 10 July, 7 August and 18 September 2026; press release “Department of War Publishes Sixth Release of Unidentified Anomalous Phenomena Files,” 18 September 2026. Cases cited here as summarised in EarthSky’s coverage of the fifth and sixth releases (Gulf of Oman AC-130J report, 8 September 2021; six-sphere infrared video, 2025; Ruppelt talk, 26 March 1952; AAWSAP Defense Intelligence Reference Documents). Independent video analysis: Metabunk, “War.gov/UFO — Department of War Releases UAP Files,” 2026. The primary files should be consulted before any figure here is relied on.

[30] Defense Intelligence Agency, Defense Intelligence Reference Documents produced under the Advanced Aerospace Weapon System Applications program and published by the Department of War as DOW-UAP-D139 and DOW-UAP-D153 (PURSUE sixth release, 18 September 2026): “Traversable Wormholes, Stargates, and Negative Energy,” DIA-08-1004-004, 6 April 2010 (Equation 8, Casimir plate spacing; Equation 9 and Table 2, negative equivalent mass; §II-C, appearance of a throat; §III-B, laboratory sources); “Quantum Tomography of Negative Energy States in the Vacuum,” DIA-08-1102-007, 11 January 2011 (balanced homodyne detection of sub-vacuum fluctuations). Author names are redacted in the released copies.

[31] Einstein, A., and Rosen, N. “The particle problem in the general theory of relativity.” *Phys. Rev.* 48 (1935): 73. Gao, P., Jafferis, D. L., and Wall, A. C. “Traversable wormholes via a double trace deformation.” *JHEP* 12 (2017): 151. Maldacena, J., Milekhin, A., and Popov, F. “Traversable wormholes in four dimensions.” arXiv:1807.04726 (2018). Jafferis, D., et al. “Traversable wormhole dynamics on a quantum processor.” *Nature* 612 (2022): 51–55; the interpretation of that experiment is debated. Squeezed light in gravitational-wave detectors: Tse, M., et al. *Phys. Rev. Lett.* 123, 231107 (2019). First detection: Abbott, B. P., et al. *Phys. Rev. Lett.* 116, 061102 (2016).

[32] Staged Z-pinch. Publications as listed by the developer: Rahman, H. U., Wessel, F. J., and Rostoker, N., *Phys. Rev. Lett.* 74, 714 (1995); Rahman et al., *Phys. Plasmas* 11, 5595 (2004); *J. Plasma Phys.* 75, 749 (2009); *Astrophys. Space Sci.* 323, 51 (2009); *Phys. Plasmas* 19, 122701 (2012); *Phys. Plasmas* 26, 052706 (2019); Conti et al., *Phys. Plasmas* 27, 012702 (2020); Ruskov et al., *Phys. Plasmas* 27, 042709 (2020) and 28, 112701 (2021). A 1997 entry is given in the source as “Physics of Plasmas 58, 367”, which does not match that journal’s volume numbering and should be checked. Patent: US 9,839,111 B2, “Staged Z-pinch for the production of high-flux neutrons and net energy.” Facilities, yields, roadmap, science team and advisory board: MIFTI Fusion company presentation, September 2025, cited with the company’s permission; financing terms in that document are not reproduced here. Independent corroboration of the Zebra result: APS Division of Plasma Physics 2017, UP11.125; Double-EAGLE experiment: LLNL-JRNL-2021661; company background:

Lyncean Group summary (2021); ARPA-E ALPHA award, 2015.

[33] Knuth, K. H., Powell, R. M., and Reali, P. A. “Estimating Flight Characteristics of Anomalous Unidentified Aerial Vehicles.” *Entropy* 21 (2019): 939. Nimitz 2004 witness and radar accounts as summarised there.

[34] Bobrick, A., and Martire, G. “Introducing physical warp drives.” *Class. Quantum Grav.* 38 (2021): 105009. Fuchs, J., Helmerich, C., Bobrick, A., Sellers, L., Melcher, B., and Martire, G. “Constant velocity physical warp drive solution.” *Class. Quantum Grav.* 41 (2024): 095013.

[35] Morris, M. S., Thorne, K. S., and Yurtsever, U. “Wormholes, time machines, and the weak energy condition.” *Phys. Rev. Lett.* 61 (1988): 1446. Friedman, J., et al. “Cauchy problem in spacetimes with closed timelike curves.” *Phys. Rev. D* 42 (1990): 1915. Echeverria, F., Klinkhammer, G., and Thorne, K. S. *Phys. Rev. D* 44 (1991): 1077. Kim, S.-W., and Thorne, K. S. *Phys. Rev. D* 43 (1991): 3929. Hawking, S. W. “Chronology protection conjecture.” *Phys. Rev. D* 46 (1992): 603.

[36] “KSM Rocket Booster / Engine — FRC-EVO Maximum Efficiency,” unattributed graphic circulated on X, 2026; described here, not reproduced. LINUS: Turchi, P. J., et al., Naval Research Laboratory imploding-liner program, 1970s. Dense plasma focus with p–^{11}B: Lerner, E. J., et al., *Phys. Plasmas* 19, 032704 (2012). Shoulders, K. R., *EV: A Tale of Discovery* (1987), for the original exotic-vacuum-object claims. Neutron-producing side reactions in p–^{11}B: see Rider [27].

[37] “Plasma Buoyancy and Trans-Domain Flight: A Classroom Discussion,” April 2026, circulated under the series title “McCasland Archive Technical Series”; author not stated, and no connection to any named individual is asserted here. Atmospheric fireballs: Ohtsuki, Y. H., and Ofuruton, H. “Plasma fireballs formed by microwave interference in air.” *Nature* 350 (1991): 139. Dikhtyar, V., and Jerby, E. “Fireball ejection from a molten hot spot by localized microwaves.” *Phys. Rev. Lett.* 96, 045002 (2006). Added mass and the 2 g limit: Batchelor, G. K. *An Introduction to Fluid Dynamics*, §6.8. Oxygen absorption at 60 GHz: ITU-R Recommendation P.676. TOPAZ: flown on Kosmos 1818 and 1867, 1987. Haisch, B., Rueda, A., and Puthoff, H. E. *Phys. Rev. A* 49 (1994): 678. Energy deposition for drag reduction: Knight, D. *J. Propulsion and Power* 24 (2008): 1153. Gas cavities and drag under water: Ceccio, S. L. *Annu. Rev. Fluid Mech.* 42 (2010): 183.

[38] Steering. RF thruster concept: “Dual-Frequency RF Plasma Thruster with Solid Hydrocarbon Propellant,” unpublished student concept paper, Kevin T. Crofton Department of Aerospace and Ocean Engineering, Virginia Tech, summer 2026 (author not named in the copy seen); baseline data as cited there from Lee et al., *Scientific Reports* (2025). Magnetic-nozzle thrust steering: Imai, R., and Takahashi, K. *Appl. Phys. Lett.* 118, 264102 (2021). Ion-wind flight: Xu, H., et al. *Nature* 563 (2018): 532. Laser-induced plasma decoys: US 11,359,892 B2 (U.S. Navy, 2022). Aerial plasma images: Ochiai, Y., et al. *ACM Trans. Graphics* 35, no. 2 (2016): 17. Learned plasma control: Degrave, J., et al. *Nature* 602 (2022): 414. Brain–computer interfaces: Hochberg, L. R., et al. *Nature* 485 (2012): 372; LaFleur, K., et al. *J. Neural Eng.* 10, 046003 (2013); Willett, F. R., et al. *Nature* 593 (2021): 249. Intention and random generators: Jahn, R., et al. *J. Scientific Exploration* 14 (2000): 499 (consortium replication); Bösch, H., Steinkamp, F., and Boller, E. *Psychological Bulletin* 132 (2006): 497. Orchestrated objective reduction: Hameroff, S., and Penrose, R. *Physics of Life Reviews* 11 (2014): 39; Tegmark, M. *Phys. Rev. E* 61 (2000): 4194. The author’s earlier protocol: Ingram, B., “Efficient Traversable Wormhole Portal System,” unpublished, January 2026.

[39] Schwarzer, N. *Fluid Universe: The Way of Structured Water and its Mathematical Foundations*. Jenny Stanford Publishing, 2026. ISBN 9789815352153. Scaled metric $G_{\alpha\beta} = F[f]\cdot g_{\alpha\beta}$ within the Einstein–Hilbert action; explicit dependence of the field equations on the dimension number; non-extremal (“ever-jittering fulcrum”) variational principle; radiating coherent domains. Comments on dimensionality and scale: private communication to the author, September 2026. Earlier exposition: Schwarzer, N. *The Theory of Everything: Quantum and Relativity is Everywhere – A Fermat Universe*. Jenny Stanford Publishing, 2020. FRC tilt instability: see Tuszewski [2].

[40] Bocker, N. J. *A MAPEOGEOv2 Reconstruction of the Three-Orb Metastructure: Formal Review, Falsification Audit, and Rebuilt Geometric-Dynamical Model*. White paper, October 2026, cited with permission. Review of Revision 10.1 of this paper under the MAPEOGEOv2 physics-certification boundary (dimensional consistency, conservation, measurement agreement, falsifier survival, replay) and the PSMSL projection/observability engine; 10,000-state randomised invariant tests (seed 20261008) of the rigid SO(3) triad, the exact toroidal breathing branch, the full collapse identities and the tilted-triad angular momentum; rank/nullity audit of single-view, stereo and mechanism-augmented projections. The four corrections adopted in Revision 10.2 (Equations 5b, 7b, 9b and the §11.4 convention) are his.

Bryan M. Ingram works at the intersection of aneutronic energy, water technology, and frontier measurement. Correspondence: bryaningram.com. Views in this working paper are the author’s and do not represent any laboratory, agency, or venture named on that site.

© 2026 Bryan M. Ingram. Working paper released for circulation and critique.